BULLETIN OF THE EARTHQUAKE
RESEARCH INSTITUTE
Vol. 40 (1962), pp. 125-173

6. *Study of Elastic Shocks Caused by the Fracture of Heterogeneous Materials and its Relations to Earthquake Phenomena.*

By Kiyoo MOGI,

Earthquake Research Institute.

(Read Dec. 22, 1959; May 24, 1960; Sept. 27, 1960.——Received Dec. 28, 1961.)

Contents

1. Introduction

It has been widely believed among geophysicists[1)] that earthquakes may be caused by the fractures or the fracture-like phenomena in the earth's crust[*)]. From this point of view, it is reasonably expected that the characteristics of brittle fracture in the earth's crust have a close connexion with the earthquake phenomena. In this paper, the writer wants to show that a careful investigation of the brittle fracture of various materials gives a clear understanding of the process of earthquake occurrences.

There are many irregularities, such as cracks and faults, in the

1) M. EWING, *Geophysics and the IGY*, *Geophys. Monograph* No. 2, (1958), 186-189.
*) This is used to express the crust and the upper mantle of the earth.

earth's crust, and its physical properties differ with the location. So it is very natural to consider the earth's crust as heterogeneous material. This heterogeneity of the earth's crust is very important in understanding the characteristics of the fractures. That is, the feature of the occurrence of fractures in heterogeneous materials is quite different in various points from that in the homogeneous materials. For example, when a uniform external stress is applied to a heterogeneous material, the stress concentrates at the irregular points in the medium, and many local fractures occur at the stress concentrated points. Such local fractures do not always grow to a large scale, but are stopped by various barriers in the medium. Therefore, the probability of the occurrence of large fractures is small and minor fractures occur more frequently. Then, the special magnitude distribution of fractures in such a heterogeneous medium as rock specimens seems to be similar to that of the fractures occurring in the earth's crust. (On the other hand, minor local fractures seldom occur in a homogeneous medium, because, as soon as a crack appears, it grows to a large scale.) Thus, a study of the fracture of heterogeneous materials may provide a clue forwards the clarifying of earthquake phenomena.

In this paper, the shock type elastic waves (elastic shocks) caused by fractures in heterogeneous materials are investigated experimentally. As the statistical approach is very important in the investigation of fracture phenomenon, the elastic shocks are also investigated by a statistical method. First, the process of the successive occurrences of elastic shocks in the various materials under an increasing or a constant stress is described. Then, the relation between the generation of the elastic shocks and the degree of the brittleness of the materials is discussed. In the following sections, the magnitude distribution of elastic shocks is investigated in relation to the heterogeneity of materials. The result seems to be analogous to the magnitude distribution of earthquakes. In the last sections, the time characteristics of the occurrence of elastic shocks are investigated and compared with those of earthquakes.

From the viewpoint that elastic shocks correspond to extremely minor earthquakes, the experiment with elastic shocks may be regarded as a model experiment for earthquakes. So, based on the above mentioned results of elastic shocks, some problems in statistical seismology are discussed.

The elastic shocks caused by the fracture of solid material were measured by F. Kishinouye[2] for the purpose of investigation of earth-

2) F. KISHINOUYE, *Bull. Earthq. Res. Inst.*, **15** (1937), 785-827.

quakes. He described the process of shock occurrences in wood specimens under a flexural stress. Recently, O. G. Shamina[3] measured elastic shocks in rock fracture and found that they increase remarkably before a main destruction. Thereafter, several investigators[4] in the U.S.S.R. did research on the occurrence of elastic shocks and also related problems, mainly for the purpose of the prediction of rock burst and the fall of roofs in mines. Very recently, the frequency distribution of the magnitude of elastic shocks in the special cases of glass and pine resin was measured by S. Kōmura[5], and N. Kobayashi and H. Takeuchi[6]. However, the present writer believes that quantitative and systematic investigations have not been made until now. This is the first step in this direction.

2. Apparatus and procedure

The elastic shocks caused by the fracture of brittle heterogeneous material under some stress conditions were measured by an acoustic method. Granite, andesite, pumice, and pine resin were used as test materials. In this experiment, fractures were caused by the statical application of stress. For our purpose, it is necessary to apply the stress without appreciable mechanical noise, because the elastic shocks should be measured under very low noise level. Therefore, an ordinary type test machine (using an oil compressor or gear system) is not suitable for the present purpose, because it is very noisy. Therefore, a noiseless apparatus of a single lever type was made for this experiment.

Experimental apparatus

The schematic view of loading apparatus is shown in Fig. 1. The

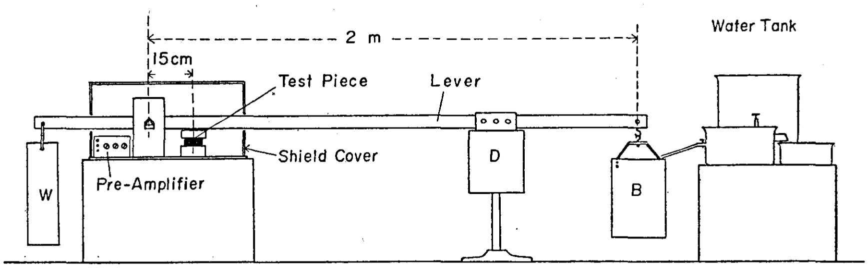

Fig. 1. Schematic view of apparatus.

3) O. G. SHAMINA, *Bull. Acad. Sci. USSR.*, No. 5 (1956), 513-518.
4) A. G. KONSTANTINOVA, *Bull. Acad. Sci. USSR. Geophysics Series*, (1959), 229-241.
5) S. KŌMURA, *Zisin (Journ. Seis. Soc. Japan)*, [ii], **8** (1955), 80-83.
6) N. KOBAYASHI and H. TAKEUCHI, Read at *the Meeting of Seis. Soc. Japan*, May,1960.

test machine of a single lever type is simple and stable, and can apply the exact stress, although it is a little difficult to handle. Increasing stress at a constant rate is applied to a test specimen by pouring water into a bucket (B) at a constant rate, and the application of a constant stress is continued by a constant weight in the bucket.

The bending test of prism specimen was carried out with the attachment shown in Fig. 2. Then, a uniform bending moment was applied to the central part of the specimen. The pumice was tested by a compression method as shown in Fig. 3. On the process of stress application, the strain of the specimen also was automatically recorded by an electric resistance strain meter and an oscillograph (the accuracy of strain measurement is of the order 10^{-6}).

The apparatus for measurement of the elastic shocks is schematically represented in Fig. 2. A pick up of the crystal cartridge type was used as a transducer of shock measurement, because it is very sensitive. It was stable in our laboratory which was at nearly constant temperature

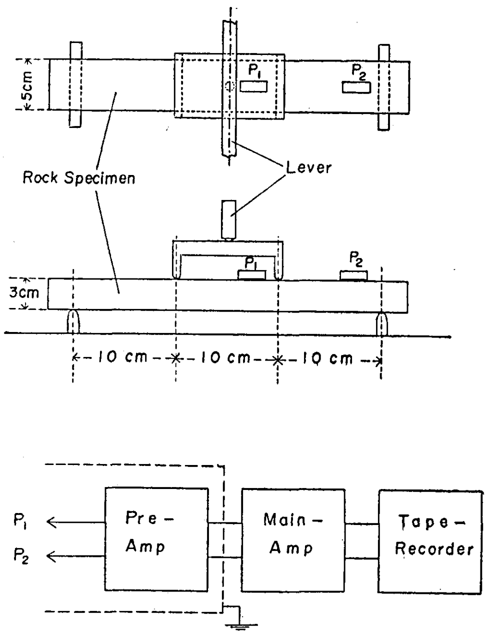

Fig. 2. upper: main part of uniform bending test.
lower: schematic diagram of shock measurement.
P_1, P_2: pick up.

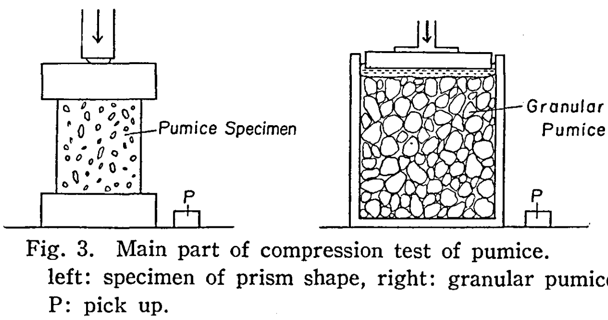

Fig. 3. Main part of compression test of pumice.
left: specimen of prism shape, right: granular pumice,
P: pick up.

and moisture. The signals were amplified by the pre- and main-amplifier and were recorded by a tape recorder, and thereafter were re-recorded by an electromagnetic oscillograph for the purpose of various measurements. The trace amplitude is proportional to the surface displacement of the specimen. One transducer was set on the test specimen, and another was set on the ground at a short distance from the specimen. By a comparison of these two records, external mechanical noises were able to be discriminated from signals. To avoid external disturbance, the experiments were carried out in the second basement of our institute under a very calm condition late at night. Thus, highly sensitive measurements of elastic shocks were attained.

Test specimens

From the microscopic point of view, the crystalline rocks should generally be considered as heterogeneous brittle materials. In the present experiment, the following samples were used as test materials.

(1) Granite $G(M_1)$, (Man-nari, Okayama Pref.)
(2) Granite $G(I_2)$, (Inada, Ibaragi Pref.)
(3) Granite $G(K_2)$, (Kitagi-sima, Okayama Pref.)
(4) Andesite $A(M_1)$, (Manazuru, Kanagawa Pref.)
(5) Andesite $A(K_1)$, (Kitakanraku, Gunma Pref.)
(6) Pumice (A), (****)
(7) Pumice (B) (granular state), (Asama Volcano, Nagano Pref.)

The specimens of granite and andesite ($3\,cm \times 5\,cm \times 35\,cm$) were cut off from a mass ($1m \times 1m \times 1m$) by a diamond cutter and the surfaces of the specimen were well polished. The density, the supersonic velocity and the bending strength were equal in the test pieces each of which were cut from a single block. These specimens were presented for a uniform bending test. The pumice was presented for a compression test as the prisms of $4cm \times 2.5cm \times 2.5cm$ or as the granular specimens which were packed in a cylindrical metal case (Fig. 3). The physical constants of these rock specimens are given in Table 2 in Section 4 and the chemical composition reported on the same kind of rock specimens is represented in Table 1.

The microphotographs of the specimens are shown in Fig. 36. From these photographs, we can see that these materials are remarkably heterogeneous in a microscale. In a later section, the degree of heterogeneity of the materials will be compared with the characteristics of the generation of elastic shocks caused by local fractures in the medium.

As the dimensions of the local fracture region are estimated to be from 0.1mm to 5mm, the structure of the materials should be examined on a similar scale. That is, the structure of these pumice specimens is

Table 1. Chemical composition of rock samples[7].

	Granite G(M_1)	Granite G(I_2)	Granite G(K_2)	Andesite A(M_1)
SiO_2	72.29	72.10	75.74	58.56
Al_2O_3	13.68	14.63	12.78	19.94
FeO	3.34	2.83	2.20	6.48
CaO	1.64	2.04	1.66	8.84
MgO	0.33	0.50	0.53	1.88
MnO	0.09	0.09	0.06	0.26
Na_2O	4.80	3.62	3.67	3.74
K_2O	3.16	3.83	3.40	0.39

very porous and extremely irregular. The granite samples have also a heterogeneous structure which holds many defects, such as crystal boundaries and micro-cracks. Typical andesite A(M_1) is almost similar to the granite in such structure, but the andesite A(K_1) shows a nearly uniform, fine crystal structure. Thus, these rock specimens are heterogeneous, more or less, and the degree of heterogeneity among the present materials is highest in the pumice, and the granite are next one. Besides these, in order to compare with the results of the above mentioned heterogeneous materials, the pine resin and the glass were presented for tests as examples of homogeneous brittle materials.

Stress distribution in bending test pieces

In the present experiment, the stress was applied to specimens mainly by means of uniform bending, as shown in Fig. 4. The uniform bending moment in the central part $\overline{bc}$ in the specimen is given as

$$M = \frac{1}{2} Fl \, (\text{kg cm}) \,, \tag{2-1}$$

where F is an applied load and l is a length of $\overline{ab}$ (or $\overline{bc}$). The bending stress σ_B at the outer surface of prism specimens is

$$\sigma_B = \frac{6M}{bh^2} = \frac{3Fl}{bh^2} (\text{kg/cm}^2) \,, \tag{2-2}$$

where b expresses the width of the prism and h expresses its thickness.

7) "Honpōsan-kenchikusekizai", 1922.

Then, the bending strength S_B is given as

$$S_B=\frac{6M_m}{bh^2}=\frac{3F_m l}{bh^2}\,(\text{kg/cm}^2)\;, \tag{2-3}$$

where M_m is the maximum bending moment and F_m is the maximum load. σ_B and S_B represent the stress and the strength respectively in the case of perfectly elastic material. However, the actual stress in the rock specimens and their actual strength are smaller than σ_B and S_B, because the non-elastic deformation takes place in a later stage of deformation. Fig. 5 is an example of the stress-strain curve of a rock

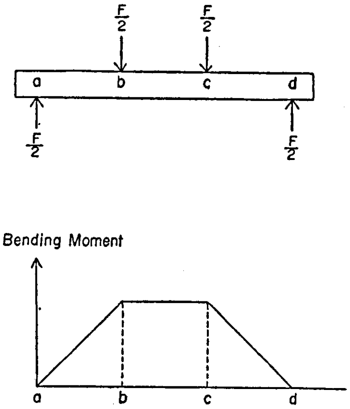

Fig. 4.

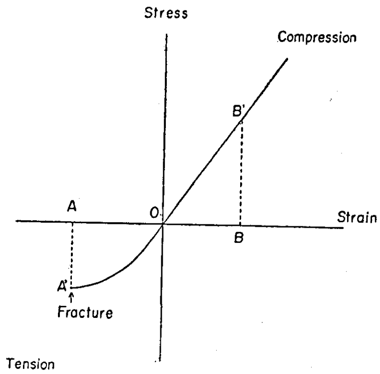

Fig. 5. A stress-strain curve of rock specimen.

specimen. If the strain distributes linearly in the direction of thickness in the bending specimen, the curve represents the stress distribution in that direction. Thus, the stress distribution in the bending specimen is not simple[8], but the calculated values σ_B and S_B are used in the following discussion as approximate values of stress and strength in the bending test. In rocks and concretes, the tensile strength is about one-tenth of the compressive strength, so the fractures caused by a bending stress occur only in the tensile side and the bending test is carried out instead of the tensile test. Furthermore, as the shear strength of rock is greater than the tensile strength under atmospheric pressure, tensile fracturing will occur also with the application of pure shear stress[9]. Accordingly, the results of the present experiment on bending stress will be also applied to the case of the shearing stress

8) M. HAMADA, *Zairyō-shikenhō*, (1954).

9) J. HANDIN, D. V. HIGGS, and J. K. O'BRIEN, *Geol. Soc. Amer.*, *Memoir* **79** (1960), 245-274.

application.

Next, the writer wants to point out that the spatial distribution of stress is an important factor in the fracturing process, because it seems to have the close relation to the characteristics of the generation of elastic shocks, as immediately seen in the following sections. In the present discussion, the stress distribution is characterized by the degree of the spatial variation of stress in the dimensions of a micro-fracture which is, as mentioned before, in the range of 0.1mm to 5mm in the present experiment. Therefore, stress distribution which changes remarkably in such a scale is not regarded as uniform. Such a viewpoint on the stress distribution is different from the ordinary expression in applied mechanics. For example, the stress distribution in a homogeneous specimen under a bending stress (not uniform in the ordinary sense) is regarded as being approximately uniform in the present discussion.

3. The patterns of occurrences of elastic shocks

When the bending stress applied to a rock specimen increases gradually, the rupture of the rock specimen occurs at the ultimate stress in a whole section. If the specimen is of a heterogeneous material, a number of local fractures will take palce in the process of the stress application. Furthermore, if these fractures are brittle, they might be accompanied by elastic waves of the shock type (elastic shocks). Actually, many elastic shocks were observed under the stressed condition by the above mentioned acoustic method (Fig. 39). The experiments were carried out under increasing stress and constant stress.

(1) *Increasing stress at a constant rate*

In the present experiment, the bending stress increases with the constant rate (5.63 kg/cm^2 min). The frequency of the elastic shocks in this experiment is the number of shocks whose trace amplitude is larger than 4mm. The frequency curves of elastic shocks in the granite, andesite, and pumice specimens are represented in Fig. 6 (the curves indicate the mean curves of several tests respectively, except in the case of the pumice). A record of the elastic shocks is shown in Fig. 7. According to that record, their amplitude is at its maximum at the initial motion and suddenly decreases with time, and the vibration periods of the waves were measured as being ($10^{-2}\sim10^{-4}$ sec). Then the wave energy which disperses as the form of an elastic shock was estimated to be approximately 10 ergs for an elastic shock of the

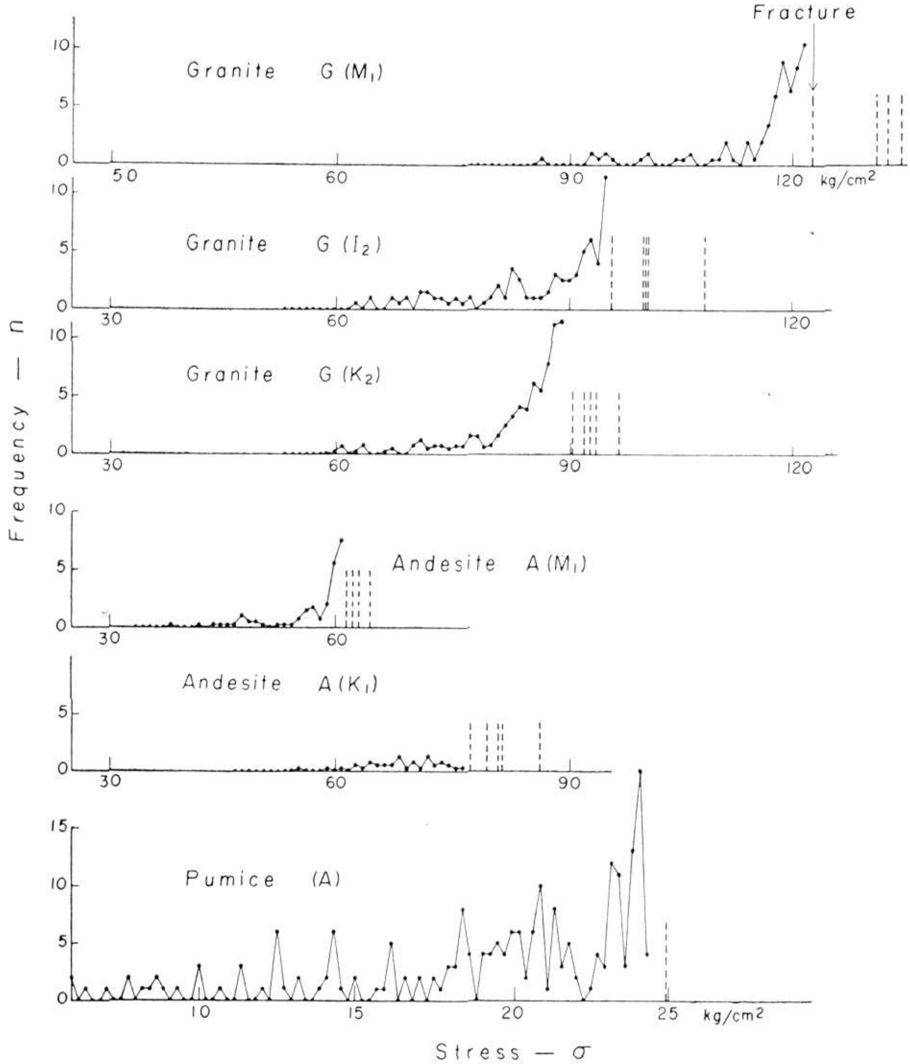

Fig. 6. Mean frequency curves of elastic shocks under the increasing stress at a constant rate.
Granite and Andesite: application of bending stress (stress rate: 5.63 kg/cm² min),
Pumice: application of compressive stress (stress rate: 1.35 kg/cm² min).

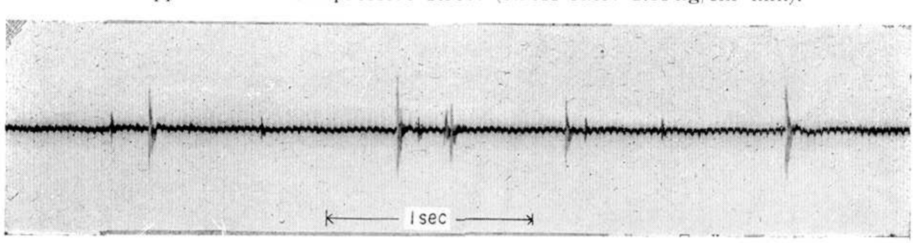

Fig. 7. Record of elastic shocks.

maximum trace amplitude 20mm. The relative value of the wave energy (W_s) of successive shocks per unit time was calculated by summing up the square of the maximum trace amplitude of each elastic shock. So we have

$$W_s = k\Sigma a^2 ,$$

where k is a constant and a is the maximum trace amplitude of an elastic shock.

Figs. 8 and 9 show frequency curves of elastic shocks and the

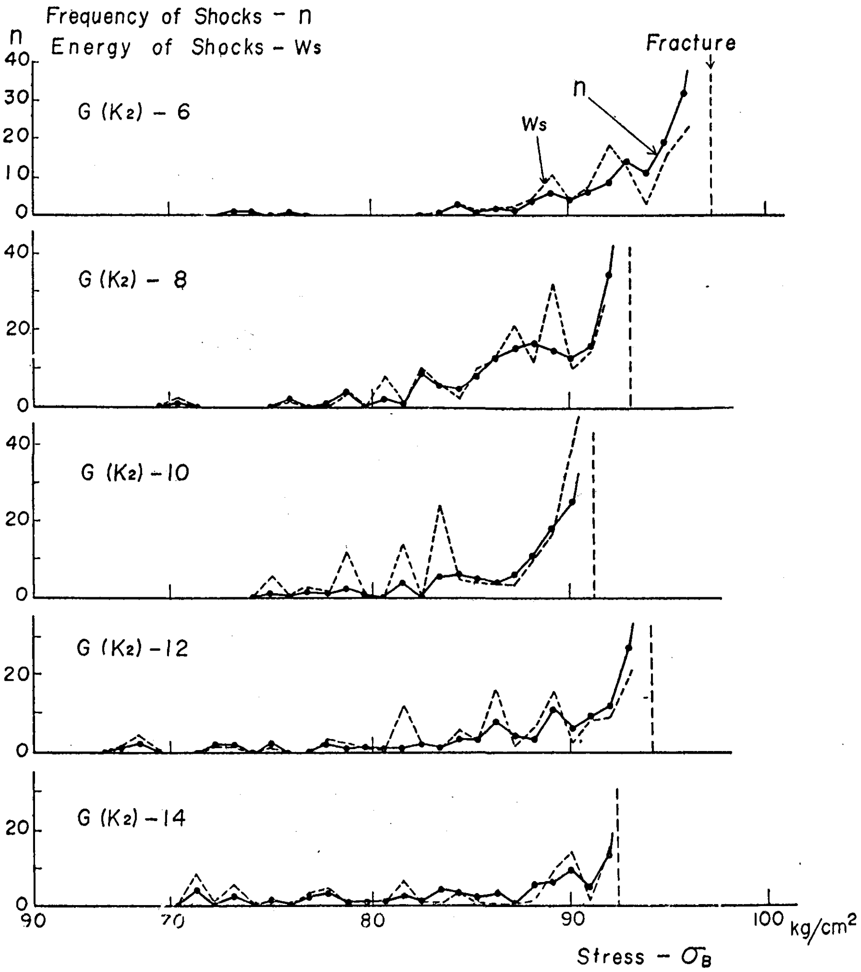

Fig. 8. Frequency curves of elastic shocks and changes of their energy under the increasing stress in Granite G(K_2) specimens. The stress rate is 5.63 kg/cm² min. The scale of energy is conventional.

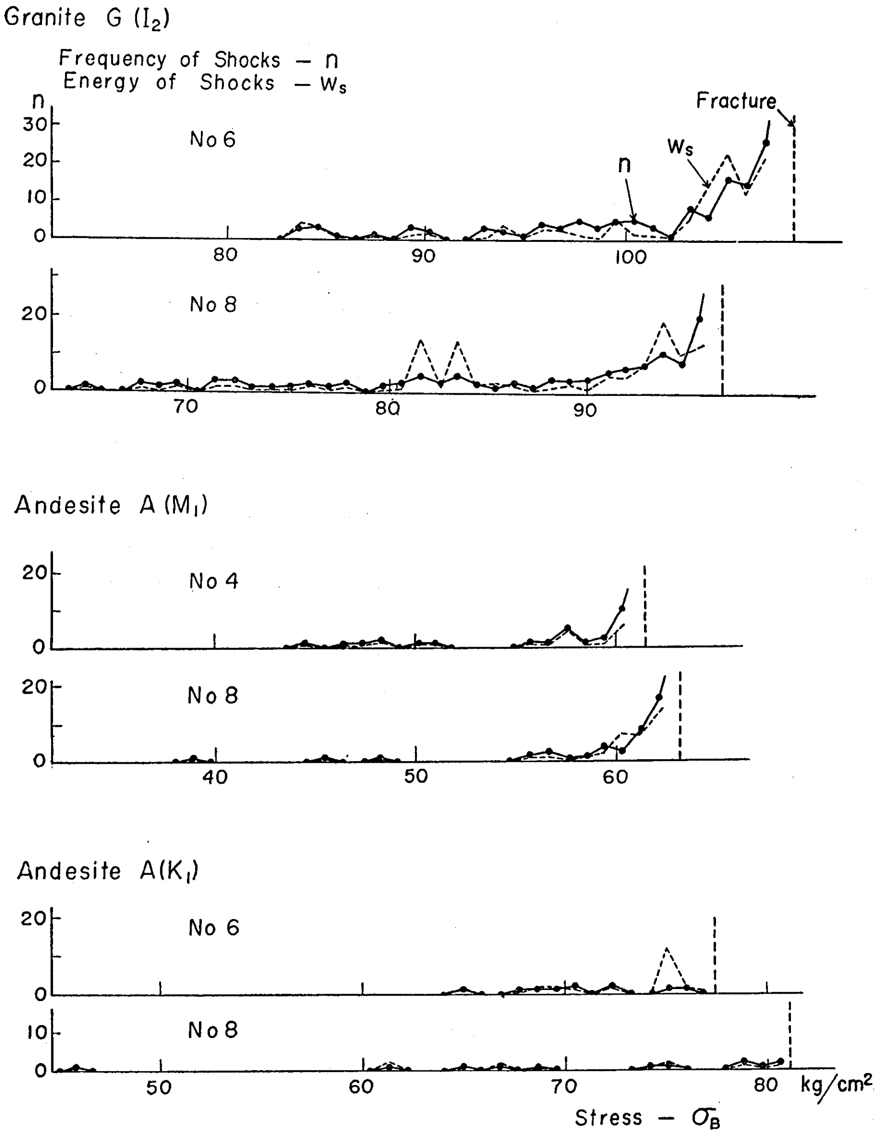

Fig. 9. Frequency curves of elastic shocks and changes of their energy under the increasing stress ($G(I_2)$, $A(M_1)$, and $A(K_1)$). The stress rate is 5.63kg/cm² min. The scale of energy is conventional.

changes of the sum of their wave energy per unit time. According to these results, the pattern of occurrences of elastic shocks is quite similar in all rock specimens of the same kind. That is, in the case of granite specimens, the elastic shocks begin to take palce at the middle or later stage and increase abruptly just before the rupture of the specimen. The sum total of wave energy of elastic shocks per unit time, also, changes in parallel with the frequency.

The pattern of successive occurrences of elastic shocks under an increasing stress at a constant rate seems to be composed of the following stages (Fig. 10).

Stage (1) In this stage, elastic shocks seldom occur and the stress-strain relation is linear (elastic deformation only take palce).

Stage (2) The frequency of elastic shocks is small and they take place sporadically.

Stage (3) The occurrence of elastic shocks is remarkable and their frequency increases in proportion to the applied stress. On the other hand, the stress-strain relation deviates from the linearity, that is, the non-elastic deformation is more predominant in this stage.

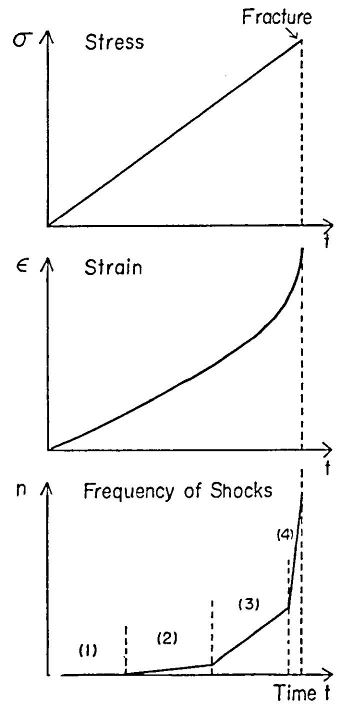

Fig. 10. Changes of the strain and the frequency of elastic shocks under an increasing stress at a constant rate for crystalline rock specimens.

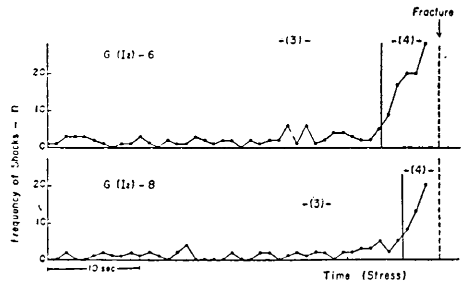

Fig. 11. Frequency curves of elastic shocks just before the rupture of granite specimens under the increasing stress at the constant rate (5.63 kg/cm^2 min). (3): Stage (3), (4): Stage (4).

Stage (4) In the last stage, just before the rupture of a specimen, the frequency of elastic shocks increases more rapidly and they occur in succession. Microscopically, the main rupture is considered to begin in this stage (Fig. 11).

The above mentioned pattern of occurrences of elastic shocks is typical in crystalline rocks. In the case of a typical andesite ($A(M_1)$), the pattern is also similar to that of granite, although the frequency of elastic shocks is smaller as compared with the latter case. However, in $A(K_1)$ specimen of an extraodinary type of andesite, an increase in elastic shocks is seldom seen before the main rupture, and the total frequency of the elastic shocks is also very small. On the other hand, it was observed that the main rupture in such homogeneous materials as glass and pine resin took place suddenly without any preceding local fracturing. According to the microscopic observation, the structure of specimen $A(K_1)$ was also nearly homogeneous. This homogeneity seems to be attained by metamorphism.

The pumice samples were investigated, as extremely heterogeneous materials. In these specimens, the elastic shocks generate frequently even at low stress and they increase remarkably with applied stress, as represented in Fig. 6. This mode of occurrences of elastic shocks is appreciably different from that of granite specimens.

(2) *Constant stress application*

Under the continual application of constant stress, rock specimens deform gradually and some of them break down after some duration of stress application[10][11]. The elastic shocks take place also under this stressed condition. According to the result of measurements, a number of elastic shocks occurs immediately after the stress application, and thereafter their frequency decreases rapidly. However, they again begin to increase after some duration of calmness and the main rupture takes place at last (Figs. 12 and 13). Thus, the pattern of occurrences of elastic shocks under constant stress has the following three stages (Fig. 14).

Stage (I) A number of elastic shocks occurs at the beginning, and thereafter they decrease rapidly with time. This stage corresponds to the transient stage in creep deformation.

Stage (II) There are almost no elastic shocks. This stage corresponds to the steady state creep stage.

Stage (III) The elastic shocks increase remarkably and at last the main rupture takes place. Microscopically, it may be the process of the growth of main rupture. This stage corresponds to the accelerating creep stage.

The process of decrease in the elastic shocks (Stage (I)) under constant stress is regarded as the stochastic process (see Section 9). The present writer wants to name this type of elastic shock "*first-class*

10) D. GRIGGS, *Journ. Geology*, **47** (1937), 225-251.

11) C. LOMNITZ, *Journ. Geology*, **64** (1960), 473-479.

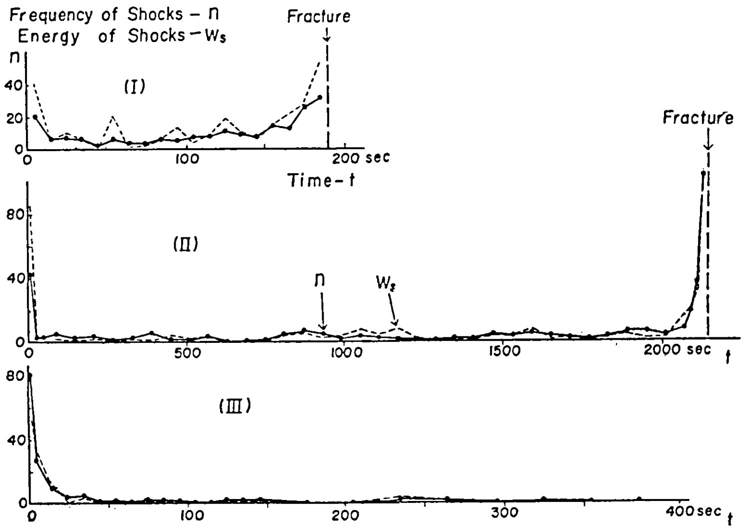

Fig. 12. Frequency curves of elastic shocks and the changes of their energy under the constant stress (Granite G(K_2)).

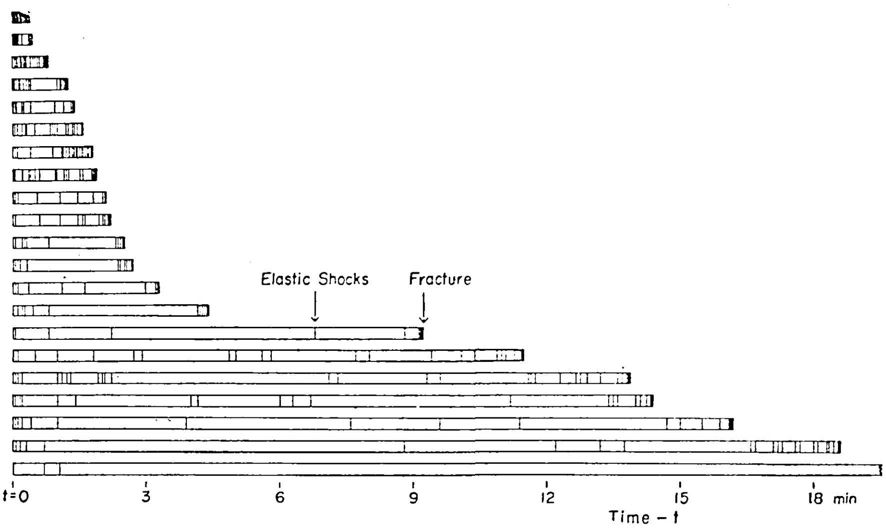

Fig. 13. Generation of the main ruptures of bending specimens and the elastic shocks caused by the constant center loading (Granite G(I_1)).

elastic shocks". The increase of elastic shocks in the last stage (III) seems to depend on the occurrence of local fractures which precede directly to the main rupture, and it is an interesting fact that preceding to the main rupture the frequency of elastic shocks increases. As such a process of the occurrences of elastic shocks is different from the above mentioned one, these shocks should be named "*second-class elastic shocks.*"

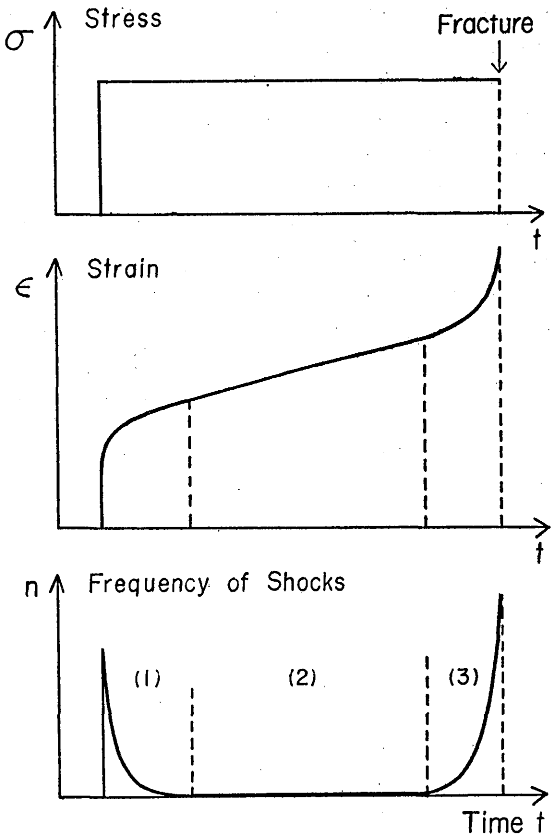

Fig. 14. Changes of the strain and the frequency of elastic shocks under a constant stress for crystalline rock specimens.

As the occurrence of elastic shocks is caused by local brittle fractures, the above mentioned results give a clue to clarifying the mechanism of deformation in the creep of rock. For example, E. C. Robertson[12], based on creep measurement under high pressure, deduced indirectly the conclusion that the mechanism of transient creep was related to the occurrence of micro-fractures in the rock specimens. The remarkable generation of local fractures

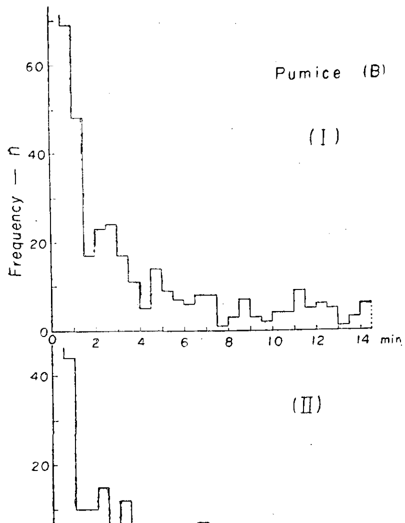

Fig. 15. Frequency histograms of elastic shocks under the constant stress for the granular pumice specimens. The constant compression stress is 0.056 kg/cm².

12) E. C. ROBERTSON, *Geol. Sec. Amer., Memoir* **79** (1960), 227-244.

in the transient creep stage (Stage (I)) was experimentally verified by the present study.

Next, the frequency distribution of elastic shocks under a constant stress in the granular pumice specimens is represented in Fig. 15. The elastic shocks occur frequently immediately after the application of constant stress and thereafter decrease with time. The process is similar to the above mentioned Stage (I) and it will be discussed again in the later section.

In such homogeneous materials, as glass and pine resin, no elastic shock occur, except that caused by the main rupture.

4. The brittleness of rocks and the generation of the elastic shocks

Since the occurrence of the elastic shocks seems to be caused by the abrupt release of the strain energy at the moment of brittle fracture, they should have some connexion with the brittleness of the materials. So, in the present section, the brittleness of the rocks is discussed with special reference to the elastic shocks. When an increasing stress is applied to various materials, the typical curves of the strain-time relation are shown in Fig. 16. The upper ones are the elastic strain curves and the middle ones are the non-elastic strain curves, and then lower ones are the frequency curves of elastic shocks which occur inside the materials during deformation. Thus, various materials seem to be classified, as follows.

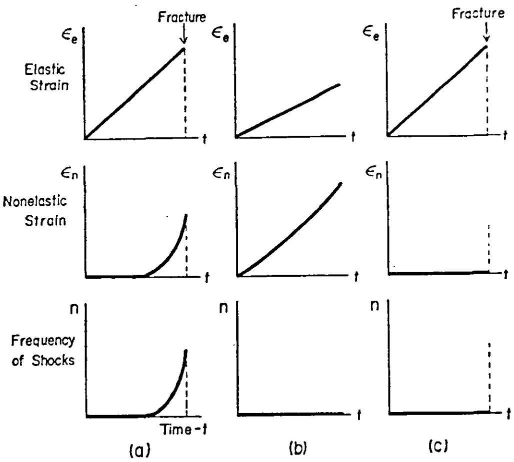

Fig. 16. Changes of elastic strain, non-elastic strain and frequency of elastic shocks under an increasing stress at a constant rate.
(a): heterogeneous brittle material,
(b): homogeneous or heterogeneous plastic material,
(c): homogeneneous brittle material.

Type (a): The heterogeneous brittle materials (example: granite in room temperature and atmospheric pressure).

Type (b): {The heterogeneous / The homogeneous} plastic materials (plastics).

Type (c): The homogeneous brittle materials (glass).

Therefore, whether or not the elastic shocks occur with the increase in the non-elastic strain, can be a appropriate measure to distinguish the difference between the brittle materials and the plastic materials (of heterogeneous structure).

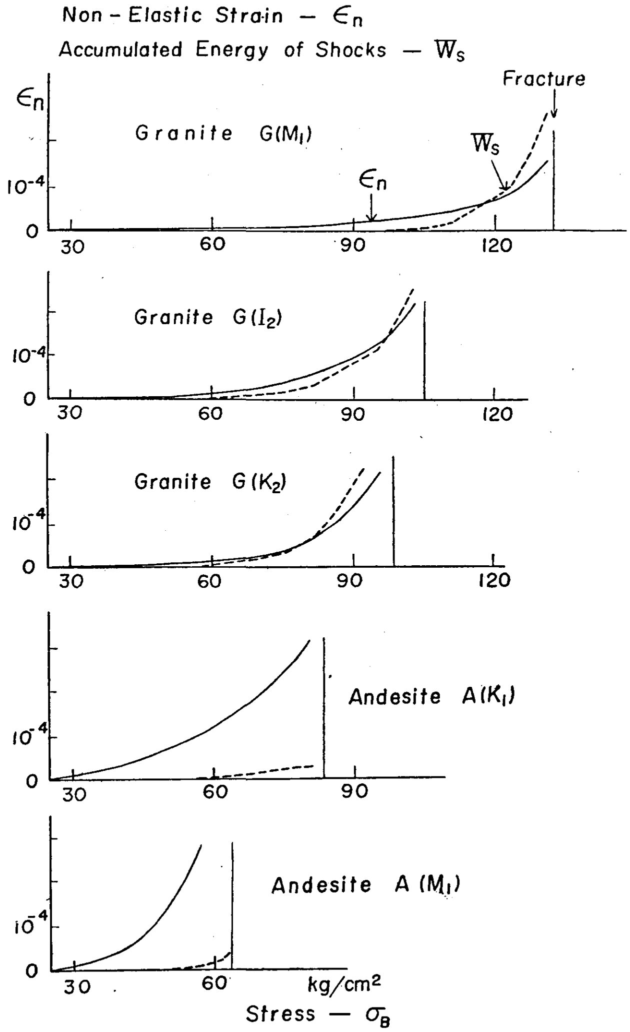

Fig. 17. Relation between the non-elastic strain and the energy of elastic shocks under the increasing stress at a constant rate. The scale of energy is conventional.
full line: non-elastic strain curve.
broken line: curve of accumulated energy of elastic shocks.

Here, to express quantitatively the brittleness of the heterogeneous materials, such as rocks, the ratio of the total energy of the elastic shocks to the total energy worked for the non-elastic deformation is introduced. But, to simplify the calculation for making the ratio, the following quantity B is used for approximation (The present writer wants to call this "*degree of brittleness*").

$$B=\frac{2W_{ef}}{\varepsilon_n S}$$

where W_{ef} is the total energy of the elastic shocks per unit volume, ε_n the total non-elastic strain, and S the maximum stress (the fracture strength). For several rocks, the relation between the non-elastic deformation and the occurrence of the elastic shocks is represented in Fig. 17. According to the result, the granite specimens are typical materials of Type(a), but the andesite ones are intermadiate, between Type(a) and Type(b). The degree of brittleness B in these rocks was calculated, as shown in Table 2. It is worth while noticing that the B value of the

Table 2. The degree of brittleness and other physical properties of various rocks. These values are the mean in several test pieces.

Rock specimen		Granite $G(M_1)$	Granite $G(I_2)$	Granite $G(K_2)$	Andesite $A(K_1)$	Andesite $A(M_1)$
Flexural strength (kg/cm²)		130.1	100.7	93.2	81.2	62.4
Supersonic wave bar velocity (km/sec) (longitudinal)		4.96	4.03	4.12	2.90	3.02
Young's modulus (kg/cm²)		38×10^4	28×10^4	23×10^4	10.3×10^4	6.7×10^4
Non-elastic ultimate strain		1.34×10^{-4}	2.18×10^{-4}	2.06×10^{-4}	3.15×10^{-4}	2.30×10^{-4}
Frequency of elastic shocks from a specimen		92	113	110	12	31
Energy of elastic shocks from a specimen (ergs)	a)*	810	580	640	105	95
	b)*	1590	615	760	152	81
Degree of brittleness (×V†)	a)*	0.093	0.053	0.067	0.008	0.013
	b)*	0.183	0.056	0.080	0.012	0.011

*) a): the energy of an elastic shock is assumed to be proportional to a^2,
b): it is assumed to be proportional to a^3.
†) V: the volume of stressed region in a specimen.

granite specimens is about ten-times that of the andesite.

The brittleness of material in the earth's crust may have some relation to the seismicity in the region. Although rocks are remarkably brittle under atmospheric pressure and in room temperature, they become ductile with an increase in pressure and temperature. Therefore, brittle fracturing in a general sense will be unable to take place in the deep part of the earth's mantle[13)14)] and the transition from brittle to ductile state in the rocks also will give rise to an interesting problem.

5. The magnitude distribution of elastic shocks (1)

The magnitude distribution of elastic shocks is an important subject in the statistical investigation of the fracture phenomenon and it seems to be closely related to the similar problem in earthquake phenomena.

With respect to earthquakes, Ishimoto-Iida's statistical relation[15)] between the maximum trace amplitude of earthquakes and their frequency is well known, that is,

$$n(a)da = ka^{-m}da, \tag{5-1}$$

where a is the maximum trace amplitude of earthquakes, $n(a)da$ is the number of earthquakes having a maximum trace amplitude a to $a+da$, and k and m are both constants. As will be mentioned in a later section, the exponent m is $1.5\sim2.0$[16)] in many cases, except in some volcanic earthquakes. As to the elastic shocks generating inside the rock specimens, whether or not the above mentioned statistical equation

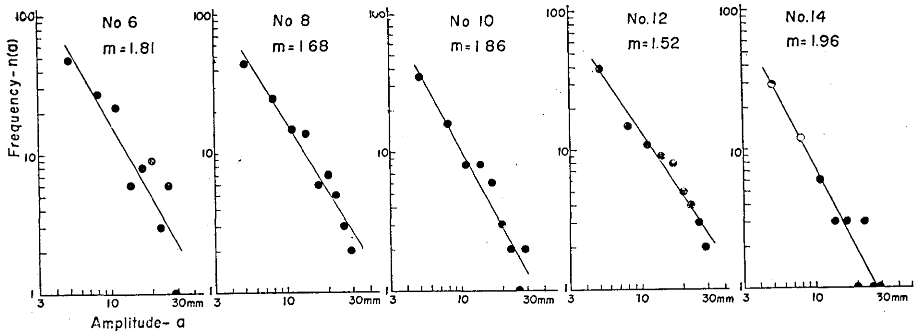

Fig. 18. Frequency distributions of maximum trace amplitude of elastic shocks in each specimen (Granite G(K_2)).

13) E. OROWAN, *Geol. Soc. Amer., Memoir* **79** (1960), 323-345.
14) D. GRIGGS and J. HANDIN, *Geol. Soc. Amer., Memoir* **79** (1960), 347-364.
15) M. ISHIMOTO and K. IIDA, *Bull. Earthq. Res. Inst.*, **17** (1939), 443-478.
16) Z. SUZUKI, *Sci. Rep. Tōhoku Univ., Ser.* 5, *Geophysics*, **5** (1953), 177-182; **6** (1955), 105-118; **10** (1958), 15-27 ; **11** (1959), 10-54.

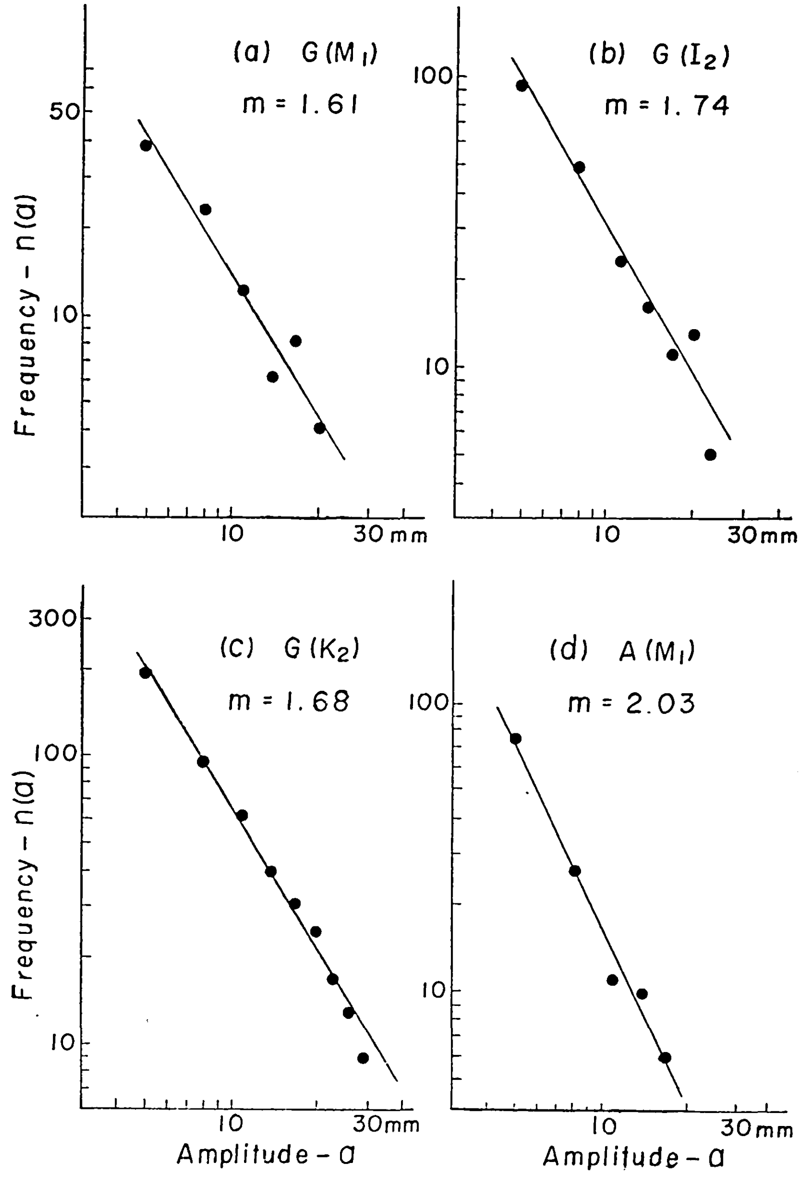

Fig. 19. Frequency distributions of maximum trace amplitude of elastic shocks.

(a), (b), (c): granite specimens under the increasing stress.
(d): andesite specimens under the increasing stress.

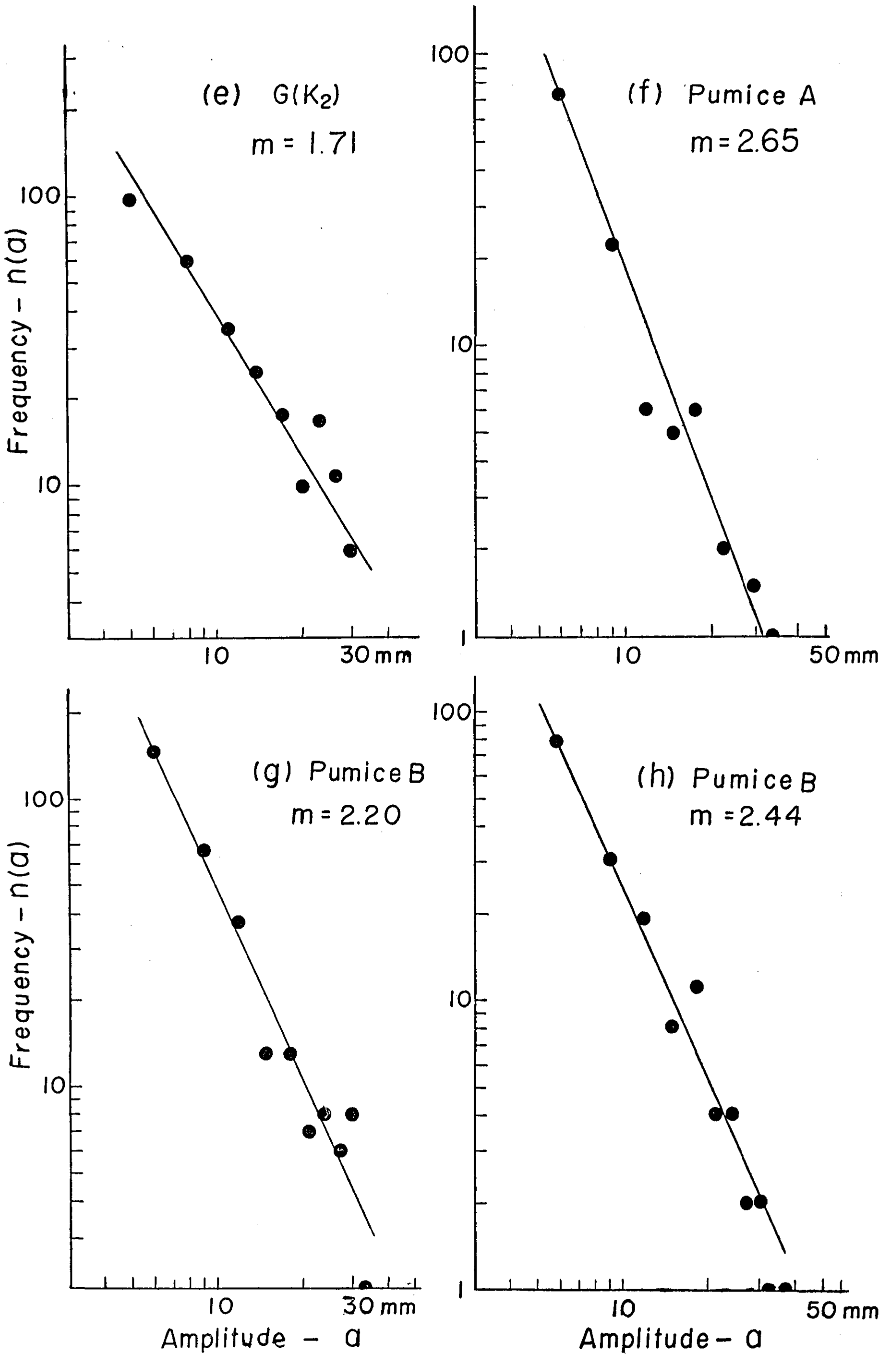

Fig. 19. (e): granite specimen under the constant stress.
(f), (g): pumice specimens under the increasing stress.
(h): pumice specimen under the constant stress.

also is satisfied, is investigated in this paper. The relation between the maximum trace amplitude of elastic shocks and their frequency is represented in Figs. 18 and 19. The results indicate that the magnitude distribution of the elastic shocks generating inside the strained rock specimens also satisfies Ishimoto-Iida's equation obtained for earthquakes. Furthermore, it is also worth while noticing that the exponent m of the elastic shocks of the granite specimens is almost the same as in earthquakes.

Table 3. Frequency distribution of maximum trace amplitude of elastic shocks in various specimens.

Trace amplitude (mm)	Granite $G(K_2)$*					
	No. 6	No. 8	No. 10	No. 12	No. 14	Total
4- 6	48	44	35	39	29	195
7- 9	27	25	16	15	12	95
10-12	22	15	8	11	6	62
13-15	6	14	8	9	3	40
16-18	8	6	6	8	3	31
19-21	9	7	3	5	1	25
22-24	3	5	2	4	3	17
25-27	6	3	1	3	0	13
28-30	1	2	2	2	2	9
Exponent m in Eq. (5-1)	1.81	1.68	1.86	1.52	1.96	1.68

Trace amplitude (mm)	Granite* $G(M_1)$	Granite* $G(I_2)$	Andesite* $A(M_1)$	Granite† $G(K_2)$
4- 6	38	92	75	99
7- 9	23	48	26	61
10-12	12	23	11	35
13-15	6	16	10	25
16-18	8	11	6	18
19-21	4	13		10
22-24		5		17
25-27				11
28-30				6
Exponent m in Eq. (5-1)	1.61	1.74	2.03	1.71

*) increasing stress
†) constant stress

(to be continued)

Table 3. (continued)

Trace amplitude (mm)	Pumice A*	Pumice B [large grained 10～20 mm]				Pumice B {fine grained 3～5 mm} No. 4*
		No. 1*	No. 2*	No. 3†	Total	
5- 7	73	119	145	78	337	56 (6-7 mm)
8-10	22	49	66	30	145	63
11-13	6	16	37	19	72	43
14-16	5	16	13	8	37	25
17-19	6	11	13	11	35	12
20-22	4	4	7	4	15	7
23-25	0	4	8	4	16	12
26-28	3	4	6	2	12	5
29-31	0	0	8	2	10	2
32-34	1	1	2	1	4	2
35-37				1		2
Exponent m in Eq. (5-1)	2.65	2.38	2.20	2.44	2.31	2.33

*) increasing stress
†) constant stress

It is easily seen that such a magnitude distribution of elastic shocks is related to the mechanical structure of the materials. To clarify the problem, similar experiments were carried out on other different materials. The pumice is very porous and extremely heterogeneous in its structure. When the cubic test specimens and the granular samples of pumice are compressed by statical stress, a remarkably large number of elastic shocks caused by micro-fractures occur. The magnitude of elastic shocks in this case, also, satisfies the statistical equation (5-1), but the exponent m (2.2～2.7) is larger than those of the granite and andesite specimens (Fig. 19 (f), (g), (h)).

Next, the homogeneous materials, such a glass and pine resin, were investigated. In such materials, elastic shocks seldom occurred before the main rupture under the increasing bending stress. This seems to be explained as follows: as soon as the first nucleus of crack generates, it grows always throughout the whole section of the specimen without any barrier. Thus, the magnitude distribution of elastic shocks in this case is different from that in heterogeneous materials.

If the applied stress fluctuates spatially, even in the homogeneous materials, such as glass and pine resin, many elastic shocks of varying magnitude occur and their magnitude distribution in some cases satisfies the above mentioned statistical equation (5–1). For example, the elastic shocks which occurred in the process of cooling the melted pine resin in a metal vessel sometimes showed the magnitude distribution represented by Eq. (5–1)[17]. In this case, the thermal stress may distribute itself very complexly at the boundary of the metal vessel and concentrate on many irregular points of that boundary.

Table 4. Relation between the frequency distribution of maximum trace amplitude of elastic shocks and the stress distribution in materials.

Test specimens	Applied stress condition	Heterogeneity of material	Stress distribution in material	Exponent m of Ishimoto-Iida's equation
Pumice (A)	compressive stress (uniform)	highly heterogeneous	highly not uniform	2.65
Pumice (B)	compressive stress (uniform)	highly heterogeneous	highly not uniform	2.38 2.20 2.44 2.33
Granite G(M_1)	bending stress (uniform)	heterogeneous	not uniform	1.61
Granite G(I_2)	bending stress (uniform)	heterogeneous	not uniform	1.74
Granite G(K_2)	bending stress (uniform)	heterogeneous	not uniform	1.68 1.71
Andesite A(M_1)	bending stress (uniform)	heterogeneous	not uniform	2.03
Andesite A(K_1)	bending stress (uniform)	nearly homogeneous	nearly uniform	*
Pine resin	bending stress (uniform)	homogeneous	uniform	*
Glass plate	bending stress (uniform)	homogeneous	uniform	*
Pine resin	thermal stress (not uniform)	homogeneous	not uniform	1.9[18] 0.5～2†
Glass plate	thermal stress (not uniform)	homogeneous	not uniform	1.70[19]

*) The exponent m may be very small ($m<1$).
†) recently obtained results for pine resin under the various stress distribution.

17) N. KOBAYASHI and H. TAKEUCHI, *loc. cit.*, 6).
18) N. KOBAYASHI, and H. TAKEUCHI, *loc. cit.*, 6).
19) S. KŌMURA, *loc. cit.*, 5).

The above mentioned experimental results are summarized in Table 4. From these results, the following important conclusion is reached: in order to possess the magnitude distribution of elastic shocks represented by Eq. (5–1), it is at least necessary that the stress distribution inside the medium fluctuates spatially, and then the fluctuation of the stress distribution inside the medium is caused both by the heterogeneity of the materials and by the applied stress which varies spatially. Furthermore, it is deduced that the exponent m in Eq. (5–1) under a comparatively uniformly applied stress may be related to the heterogeneity of the materials.

6. The magnitude distribution of elastic shocks (2)

As shown in the preceding section, the magnitude distribution of elastic shocks generated in the rock specimens satisfies Ishimoto-Iida's statistical equation (5–1). Futhermore, it is indicated that such a distribution of magnitude has a close relation to the stress distribution inside the materials, as follows. (i) When the material is homogeneous and the external stress is uniform, the ratio of frequency of small shocks to that of large ones is very small. (ii) If the mechanical structure of the material is remarkably heterogeneous or a non-uniform external stress is applied, small elastic shocks take place frequently as compared with the large shocks, and the magnitude distribution of elastic shocks satisfies Eq. (5–1) in some cases and the exponent m seems to increase with the degree of inequality of stress distribution in the medium.

The result is explained qualitatively by the fact that the probability —with which the growth of fracture is halted by the barriers, such as troughs of stress distribution,—is large in a remarkably heterogeneous material. However, if the following relations (6–1), (6–2) and (6–3) are assumed, Eq. (5–1) is quantitatively derived from them*.

(1) The energy E of an elastic shock is related to the amplitude a by

$$E=k_1a^\nu, \qquad (6\text{–}1)$$

where k_1 and ν are constants.

(2) An elastic shock occurs, caused by a local fracture of heterogeneous material, and its energy E is proportional to the volume V of

*) The explain of Eq. (5-1) was also tried by the following authors:
Z. Suzuki, *loc. cit.*, 16).
Y. Tomoda, *Zisin* (*Journ. Seis. Soc. Japan*), [ii], **8** (1956), 196-204.

the fracturing domain. So we have

$$V=k_2E, \tag{6-2}$$

where k_2 is a constant.

(3) The probability $f(V)dV$ of the growth of fracture being halted while the fracturing volume V increases to $V+dV$, is inversely proportional to the volume V of the fracturing domain,

$$f(V)dV=k_3\frac{\kappa}{V}dV, \tag{6-3}$$

where k_3 is a constant and κ is a degree of the spatial fluctuation of stress distribution in materials.

The assumptions (1) and (2) may be reasonably accepted. The assumption (3) is based on the following consideration. That is, the growth of fracture should be considered as a stochastic process. When the fracturing volume reaches V, the stress concentrated region V' appears around the fracturing region, and the former (volume V') is proportional to the latter (V). If we take the standpoint that the increase in fracturing volume is caused by the transition from the stressed state to the fracturing state at the stress concentrated region and the halt in the growth of the fracture is caused by the inequality of stress distribution in the related region, the above mentioned probability $f(V)dV$ should be inversely proportional to V' and proportional to the inequality κ of the stress distribution. Thus, Eq. (6-3) is obtained.

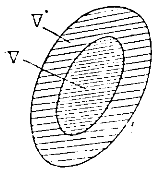

Fig. 20.
V: fracturing region.
V': stress concentrated region.

From the above assumptions (6-1), (6-2) and (6-3), Eq. (5-1) is derived in the following way. The frequency of fractures which have the fracturing volume V to $V+dV$ is expressed by $n(V)dV$. So the accumulated frequency of fractures should be

$$N(V)=\int_V^\infty n(V)dV. \tag{6-4}$$

As $f(V)dV$ is the probability that the growth of fracturing volume V is halted during the increase in small volume dV, we have

$$f(V)dV=-\frac{dN}{N}=-d[\log N(V)]. \tag{6-5}$$

On the other hand, Eq. (6-3) is

$$f(V)dV=k_3\frac{\kappa}{V}dV=k_3\kappa d(\log V). \tag{6-6}$$

Therefore, we get

$$N(V)=cV^{-k_3\kappa}, \tag{6-7}$$

where c is a constant.

Putting Eq. (6-4) into this relation, we have

$$dN=-n(V)dV=k_3\kappa c V^{-k_3\kappa-1}dV. \tag{6-8}$$

Also, putting Eq. (6-2) into Eq. (6-8), we have

$$n(E)dE=k_4E^{-k_3\kappa-1}dE, \tag{6-9}$$

where $k_4\equiv k_3\kappa c k_2^{-k_3\kappa}$.

Putting Eq. (6-1) into Eq. (6-9), we have the following equation which is the same as Eq. (5-1),

$$n(a)da=ka^{-m}\,da, \tag{6-10}$$

where $$k=\nu k_1^{-k_3\kappa}k_4,$$

and $$m=\nu k_3\kappa+1. \tag{6-11}$$

Thus, Ishimoto-Iida's statistical equation is derived from the above mentioned assumptions. According to this result, the exponent m in Eq. (5-1) has a linear relation with κ which indicates the degree of the spatial fluctuation of stress. Therefore, if the external stress is nearly uniform, the exponent m increases with the degree of heterogeneity in the material. Here the variation in the stress distribution (or the heterogeneity of the material) is considered in the scale of the dimension of local fracture (0.1mm-5mm), as mentioned in the preceding section.

7. Relation between the magnitude distribution of elastic shocks and that of earthquakes

As mentioned before, it is well known that there is a statistical relation between the maximum trace amplitude of earthquakes and their frequency at an observatory, that is, Ishimoto-Iida's relation (Eq. (5-1)). The same relation is also satisfied in the magnitude distribution of earthquakes. The exponent m in Eq. (5-1) has the same value in the both cases. On the other hand, Gutenberg and Richter[20] obtained the magnitude distribution of earthquakes by introducing the instrumental magnitude scale, and their result is essentially similar to Ishimoto-Iida's relation. According to these results, the statistical equation (5-1) is applicable to the wide range of earthquakes from large to minor. It is

20) B. GUTENBERG and C. F. RICHTER, *Seismicity of the Earth*, (1954). The constant b in their magnitude-frequency relation equals to $(m-1)$.

worth while to notice that the exponent m in Eq. (5-1) is approximately constant ($1.5\sim2$) in various cases[21)22)23)24)], except for some earthquakes of volcanic origin. However, the minute difference in the magnitude distribution in various regions was discussed by C. Tsuboi[25)] and S. Miyamura[26)] in recent years.

Earthquakes (except some volcanic earthquakes which consist of continuous trains) are divided into two groups by the value of exponent m in Eq. (5-1). The first group ($m=1.5\sim2.0$) includes general earthquakes, aftershocks, earthquake swarms and volcanic earthquakes of deep focus. The second group has larger values of m ($m=2\sim4$) and includes the volcanic earthquakes of shallow origin and the volcanic explosion earthquakes.

As mentioned above, the exponent m for various earthquakes originated from the earth's crust is nearly constant ($1.5\sim2$). Recently, a similar magnitude distribution in very small earthquakes (the energy 10^{19} ergs) had been ascertained by T. Asada[27)]. Furthermore, if the elastic shocks in crystalline rocks (their energy $1\sim10^2$ ergs) are regarded as extremely small earthquakes, it is noticeable that Eq. (5-1) is, also, satisfied and its exponent m is also similar in such minor earthquakes.

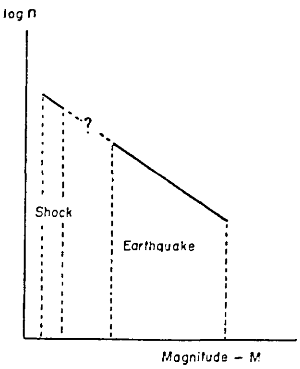

Fig. 21.

If earthquakes take place by fracturing of the earth's crust, the preceding discussion on the magnitude distribution of elastic shocks should be applicable to the earthquakes. That is, Ishimoto-Iida's relation in earthquakes indicates that the earth's crust is remarkably heterogeneous, and the heterogeneity is nearly constant anywhere in the earth's crust and is analogous to the microscopic heterogeneity of the crystalline rocks (if the applied stress in the earth's crust is to be considered nearly uniform).

A large number of volcanic earthquakes takes place directly under some active craters. Their focal depth is generally shallower than 1km.

21) B. GUTENBERG and C. F. RICHTER, *loc. cit.*, 20).
22) C. TSUBOI, *Journ. Rhys. Earth*, **1** (1952), 47-54.
23) T. ASADA and Z. SUZUKI, *Geophys. Notes*, No. 16 (1949), 1-14.
24) Z. SUZUKI, *loc. cit.*, 16).
25) C. TSUBOI, read at *the Meeting of Seis. Soc. Japan*, Oct. 1960.
26) S. MIYAMURA, *Proc. Jap. Acad.*, **38** (1962), 27-30.
27) T. ASADA, *Journ. Phys. Earth*, **5** (1957), 83-113.

Such volcanic earthquakes are called *B-type*[28]. The other type of volcanic earthquakes of deeper origin also takes place in the volcanic region and they are called volcanic *A-type* earthquakes. For both types of volcanic earthquakes, Ishimoto-Iida's relation is also satisfied, but the exponent m of the *A-type* takes ordinary values (1.5~2) and that of the *B-type* takes remarkably large values (2~4)[29][30][31][32][33]. From these results, the stress distribution in the deep region of the volcanic area seems to be not far different from the other region of the earth's crust. On the other hand, the stress distribution in the medium directly under the active crater must fluctuate spatially at a high degree. This stress condition may be caused both by the remarkable heterogeneity of the materials in the crater bottom and also the concentrated stress application by the gas intrusion or the movement of the viscous magma. Considering the fact that the exponent m in the case of pumice specimens is large (2~3), we may say that the medium in a crater bottom may consist of the clastic materials.

8. Time characteristics in the occurrences of elastic shocks (1)

The process of the occurrences of elastic shocks under stress application in various materials was described in Section 3. A more quantitative investigation on this subject is given in this section.

First, to be considered is whether the occurrence of an elastic shock influences the next shocks or not. For this purpose, the frequency distribution of time interval τ in the successive elastic shocks is examined. The results in the case of increasing stress at a constant rate are shown in Fig. 22. According to these results, the frequency $n(\tau)d\tau$ of the time intervals from τ to $\tau+d\tau$ is approximately expressed by

$$n(\tau)d\tau = he^{-\alpha\tau}d\tau, \tag{8-1}$$

where h and α are constants. From these results, it is deduced that the elastic shocks occur independently and at random. The exponent α corresponds to the probability of the occurrence of elastic shocks and varies with the stress condition. However, it should be noticed that

28) T. MINAKAMI, *Bull. Earthq. Res. Inst.*, **38** (1960), 497-544.
29) Y. TOMODA, *Zisin* (*Journ. Seis. Soc. Japan*), [ii], **7** (1954), 155-169.
30) T. MINAKAMI, *loc. cit.*, 28).
31) Z. SUZUKI, *loc. cit.*, 16).
32) S. SAKUMA, *Geophys. Bull. Hokkaidō Univ.*, **6** (1958), 1-7.
33) T. KIZAWA, *Meteorology and Geophisics*, **8** (1957) 150-169.

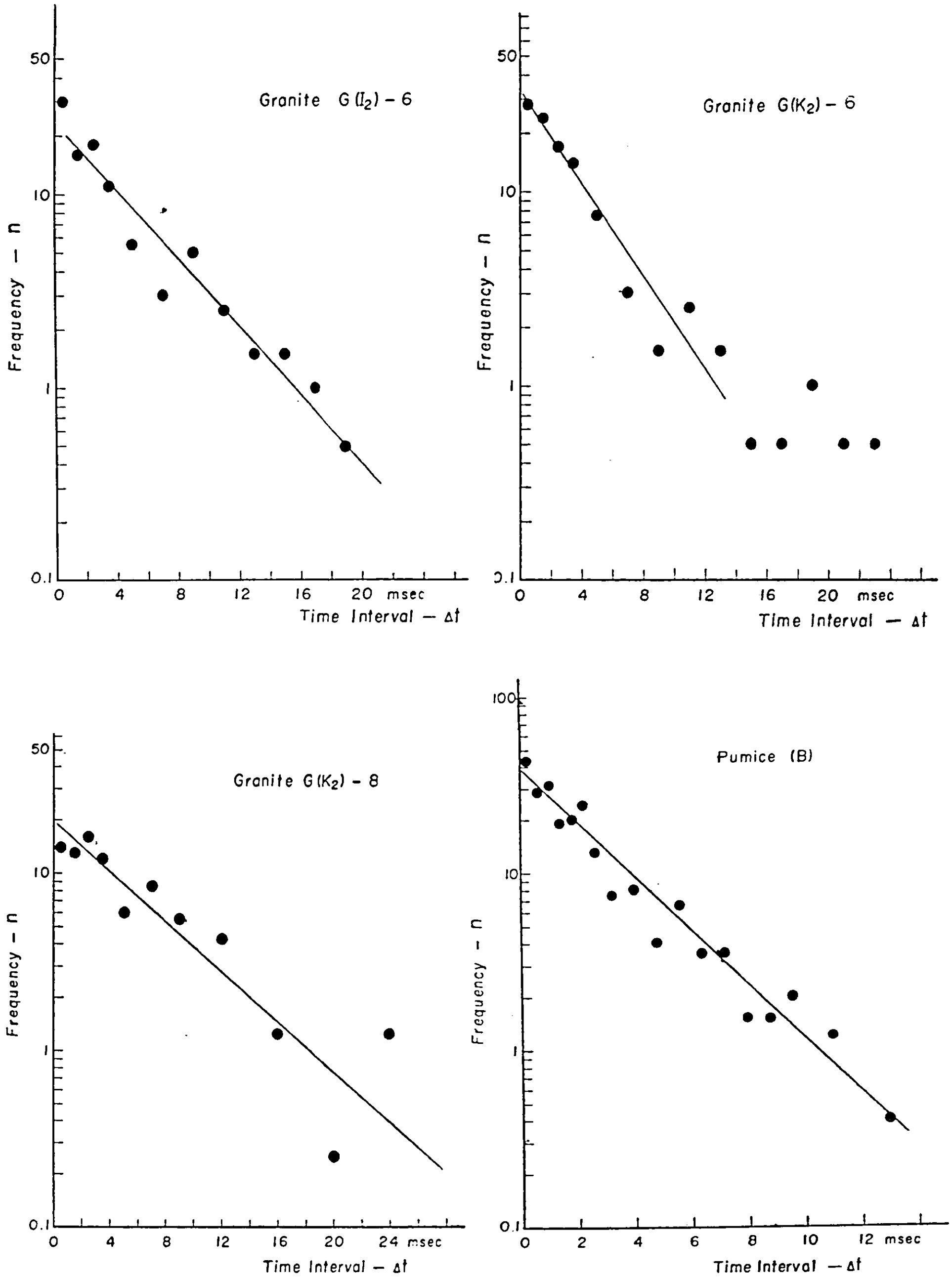

Fig. 22. Frequency distribution of time intervals of elastic shocks.

such a statistical analysis is able to be applied only to the stationary stochastic process. Therefore, if the parameters of the process in question vary remarkably and systematically, the process should be separated into several series of stationary processes. For example, Fig. 23 shows the two frequency distributions of time intervals of elastic shocks which occur in the pumice specimen under increasing stress at a constant rate. In the figure, the double circles (1) show the distribution in a later stage (stress$=17\sim24$ kg/cm^2) and the closed circles (2) show it in the early stage (stress$=10\sim17$ kg/cm^2), and the straight line shows the exponential distributions corresponding to the respective cases. Thus, although the distributions (1) and (2) are represented by the exponential function (8–1) respectively, the distribution over the whole process (stress$=10\sim24$ kg/cm^2) is not represented by Eq. (8–1), because the exponent α is not constant over the whole process. Thus, the distribution for the process which has different exponents in several stages must be represented by the curve which concaves upward in a semi-logarithmic scale.

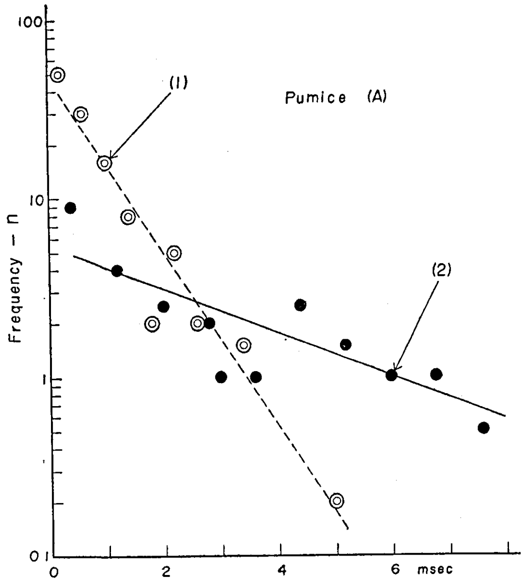

Fig. 23. Frequency distribution of time intervals of elastic shocks under the increasing stress at a constant rate.
(1): stress$=17\sim24$, (2): stress$=10\sim17$ kg/cm^2.

Next, the frequency curve of elastic shocks under a constant stress is analyzed. As mentioned in the preceding section, the frequency of elastic shocks (*first-class elastic shocks*) decreases monotonically after the stress application. The accumulated frequency curves of elastic shocks are shown in Figs. 24 and 25. Here, the accumulated frequency $N(t)$ is defined by

$$N(t)=\int_t^\infty n(t)dt, \qquad (8\text{–}2)$$

where $n(t)$ is the frequency of elastic shocks. Since the relation between

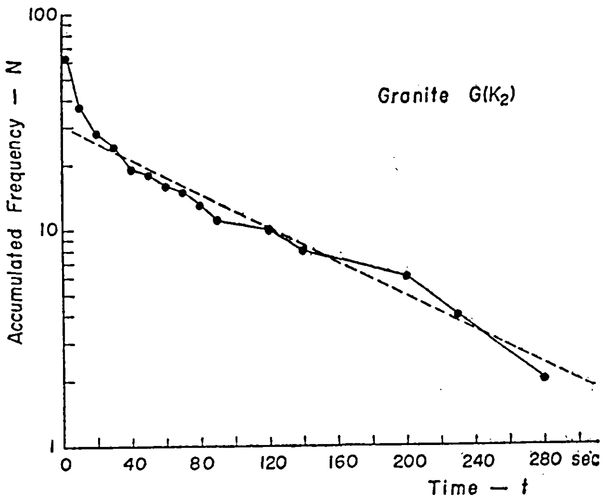

Fig. 24. An accumulated frequency curve of elastic shocks under the constant stress $\sigma_B=87\,\mathrm{kg/cm^2}$. It corresponds to the frequency curve (III) of Fig. 12.

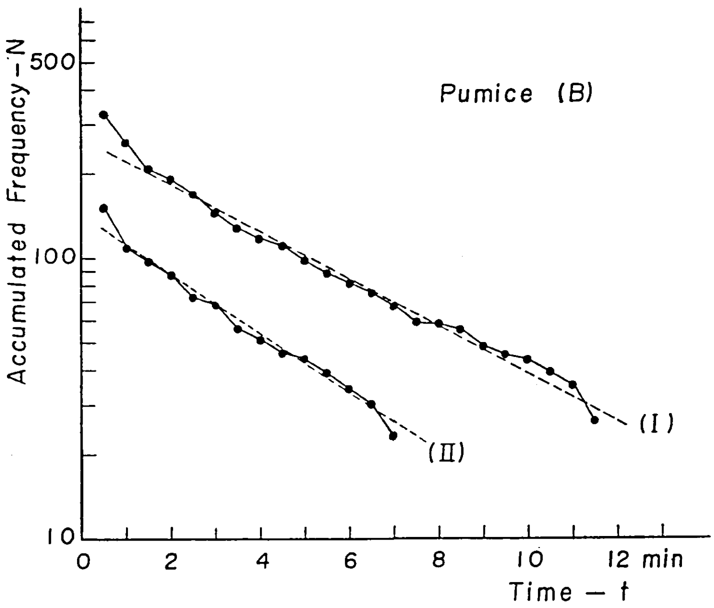

Fig. 25. Accumulated frequency curves of elastic shocks of the granular pumice under the constant stress $\sigma_c=0.056\,\mathrm{kg/cm^2}$. They correspond to the frequency curves of Fig. 15.

Table 5. Frequencies of elastic shocks in Pumice (B) specimens under constant load.

Time (min)	I		II	
	observed	calculated*)	observed	calculated*)
$0.5 \leqq t \angle 1$	69	33	44	15
$1 \leqq t \angle 2$	65	61	20	26
$2 \leqq t \angle 3$	47	46	19	20
$3 \leqq t \angle 4$	28	35	17	16
$4 \leqq t \angle 5$	19	26	7	13
$5 \leqq t \angle 6$	16	20	10	10.2
$6 \leqq t \angle 7$	14	15	11	8.0
$7 \leqq t \angle 8$	9	11.2	11	6.5
$8 \leqq t \angle 9$	10	8.6	4	5.2
$9 \leqq t \angle 10$	5	6.5	5	4.1
$10 \leqq t \angle 11$	8	5.0	2	3.3
$11 \leqq t \angle 12$	14	3.8	1	2.6
$12 \leqq t \angle 13$	11	2.9		
$13 \leqq t \angle 14$	4	2.2		

*) frequencies calculated from an exponential function.

$\log N(t)$ and t seems to be nearly linear except in the initial stage, the frequency $n(t)$ will be approximately expressed by

$$n(t)dt = n_0 e^{-\mu t} dt, \tag{8-3}$$

where n_0 and μ are constants. That is, the frequency of elastic shocks under a constant stress decreases exponentially with time, and so it is deduced that the elastic shocks occur with a constant transition probability under a constant stress, as shown in the next section.

9. Time characteristics in the occurrences of elastic shocks (2) —Analysis by the theory of the stochastic process

Recently, it has been made clear by some investigators that the generation of fractures in various materials is adequately explained as a sort of stochastic process. Since the fracture theory from such a point of view was established by M. Hirata[34] on the fracturing of glass specimens, some investigators[35][36][37] found that this theory can be applied

34) M. HIRATA, *Ōyōtōkeigaku*, Chapter 11, (1949).
35) T. YOKOBORI, *Journ. Phys. Soc. Japan*, **6** (1951), 81; **8** (1953), 265.
36) B. D. COLEMAN, *Journ. Appl. Phys.*, **27** (1956), 862-866.
37) M. HORI, *Journ. Appl. Phys. Japan*, **27** (1958), 690-698.

to the fractures of various materials, such as metals, plastics and concrete.

The present writer tried to analyze the process of the occurrences of elastic shocks in heterogeneous brittle materials, such as rocks, from the stochastic point of view. As the first step, the main fracture of rock specimens under external stress σ is discussed. The occurrences of elastic shocks caused by local fractures in heterogeneous materials should be also explained similarly, if the external stress σ is replaced by $q\sigma$, where q is the coefficient of stress concentration at irregular points in the specimen.

The time distribution of the generation of the main rupture in many specimens under constant applied stress was measured by the following experimental procedure. About one hundred specimens in the shape of prisms (the dimensions 3cm × 4cm × 15cm) were prepared. The stress application was carried out by Michaelis bending apparatus (Fig. 40). The time between the application of a constant load and the generation of the rupture was measured by the electric chronometer which was switched off automatically by a relay. The experiment was carried out with extreme carefulness so as to reduce experimental errors to a minimum. But, there remained somewhat of an error, that is, a fault caused by the fact that the test specimens were not completely uniform, as observed in the fluctuation of the supersonic velocity of the specimens. This is referred to later in the analysis of these results.

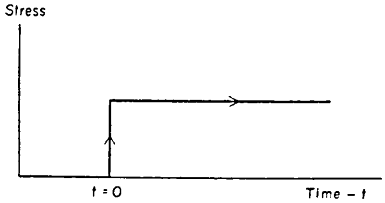

Fig. 26.

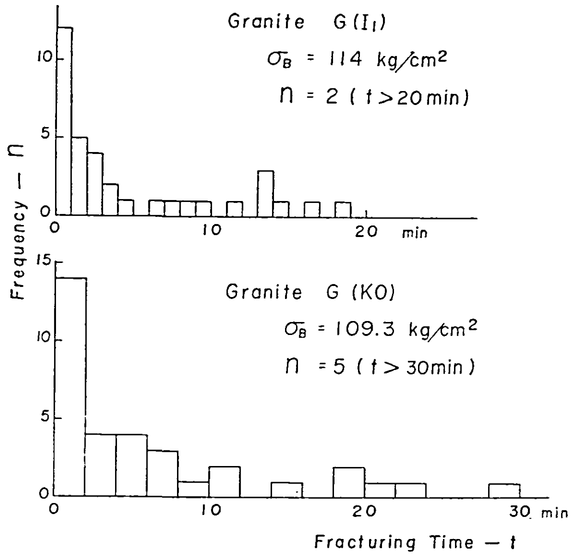

Fig. 27. Frequency histograms for fracturing time of granite specimens under the constant stress.

The frequency histograms for the fracturing time are shown in Fig. 27. The frequency

Table 6. Fracturing time under constant load.

Granite G(I_1)

Applied bending stress (σ_B) (kg/cm^2)	Specimen No.	Fracturing time (t) (min)	Supersonic bar-velocity (V) (km/sec)	Density (ρ)
114	A 3	18.63	4.12	2.612
	A 6	0.80	4.15	2.616
	A 8	1.78	4.17	—
	A 9	11.50	4.16	2.614
	A11	2.17	4.13	2.617
	A14	0.40	4.11	2.614
	B 1	0.08	4.17	2.613
	B 2	1.00	4.11	—
	B 3	14.30	4.14	2.615
	B 4	0.08	4.12	2.618
	B 6	0.48	4.12	—
	B 8	0.43	4.24	2.613
	B 9	8.60	4.08	—
	B10	0.39	4.16	2.610
	B11	6.26	4.12	—
	B13	0.03	4.07	2.612
	C 1	4.40	4.14	2.611
	C 3	1.62	4.12	2.612
	C 4	1.37	4.14	—
	C10	0.08	4.14	2.611
	C13	3.36	4.08	—
	C14	0.08	3.95	2.611
	D 2	13.31	4.22	—
	D 3	60.0	4.17	2.615
	D 6	0.82	4.11	2.613
	D 8	1.83	4.11	2.612
	D 9	1.42	4.16	—
	D12	3.27	4.10	—
	D13	0.37	4.11	2.612
	E 1	9.17	4.22	—
	E 4	104.	4.17	2.617
	E 5	13.25	4.15	—
	E 6	0.08	4.16	2.618
	E 9	2.49	4.20	—
	E10	2.67	4.17	—
	E11	16.20	4.16	2.611
	E13	0.64	4.15	—
	F 1	7.76	4.22	2.615
	F 4	0.57	4.22	2.615
	F 7	2.10	4.24	2.623
	F 9	1.92	4.25	2.617
	F11	0.05	4.13	2.610
	F13	13.83	4.16	2.609
	mean	7.75		

(to be continued)

Table 6. (continued)

Applied bending stress (σ_B) (kg/cm²)	Specimen No.	Fracturing time (t) (min)	Supersonic bar-velocity (V) (km/sec)	Density (ρ)
118	A 2	1.07	4.16	—
	A 4	0.03	4.20	—
	B 5	3.10	4.11	—
	D10	0.10	4.12	2.612
	E 3	0.25	4.20	2.611
	F12	0.05	4.15	2.610
	G 2	10.6	4.25	2.615
	G 8	1.60	4.29	2.615
	G11	0.05	4.26	2.618
	mean	1.80		
110	B 7	137.2	4.11	2.613
	C 6	0.33	4.15	2.613
	C 9	17.0	4.16	2.612
	D 1	11.0	4.16	2.615
	E 7	15.0	4.17	2.612
	F 2	109.	4.20	—
	F 5	1.0	4.21	2.614
	G 3	0.30	4.28	2.612
	G 6	2.60	4.24	2.616
	G13	7.50	4.22	2.615
	mean	30.1		
104	A 5	0.41	4.19	2.614
	C 5	2.67	4.10	2.613
	E 2	149.	4.24	2.615
	F 3	189.	4.19	2.611
	G 1	370.	4.22	2.616
	G 4	111.	4.24	2.614
	G 9	148.	4.28	2.617
	mean	140.		
	No.	Strength (kg/cm²)	V (km/sec)	ρ
	A13	113.4	4.15	2.615
	B 8	111.8	4.24	2.613
	C 2	110.8	4.14	2.614
	D 4	118.1	4.11	2.613
	D14	104.8	4.06	2.615
	E 8	112.9	4.16	2.610
	E12	116.4	4.19	2.613
	F 6	117.3	4.30	2.614
	F10	113.5	4.16	2.613
	F14	117.1	4.16	2.606
	G 7	121.6	4.28	2.615
	G10	120.2	4.20	2.613
	mean	114.8		

(to be continued)

Table 6. (continued)

Granite G(KO)*) Applied bending stress: 109.3 kg/cm²

Specimen No.	t (min)	V (km/sec)
1	3.15	4.19
3	2.88	4.21
4	4.00	4.08
6	11.58	4.17
8	7.43	4.13
11	14.48	4.19
13	0.42	4.19
14	107.93	4.24
16	29.10	4.37
18	23.97	4.31
19	0.17	4.13
21	0.18	4.28
23	0.03	4.20
24	19.52	4.26
26	11.20	4.12
28	2.03	4.31
29	0.05	4.05
31	0.65	4.29
33	0.00	4.08
34	18.73	4.29
36	0.00	4.21
38	106.57	4.19
39	0.17	4.10
41	110.35	4.24
43	5.57	4.11
44	4.05	4.26
46	2.43	4.05
48	1.45	4.22
49	20.60	4.26
51	6.10	4.20
53	0.38	4.17
54	166.	4.21
56	373.	4.31
58	0.40	4.05
59	6.77	4.17
61	4.63	4.21
63	0.97	4.21
64	0.93	4.08
66	9.00	4.07

No.	Strength (kg/cm²)	V (km/sec)
5	120	4.10
10	117	4.18
15	123.5	4.10
20	118	4.17
25	121	4.08
30	121	4.17
35	132.5	4.31
40	123.5	4.19
45	116	4.19
50	119.5	4.10
55	129.5	4.22
60	116	4.19
65	132.5	4.28

*) Granite G(KO): Komikage.

distribution is far different from a normal distribution and this fluctuation is not an experimental error, but the fluctuation is regarded as the inherent characteristic of the fracture phenomenon. According to the accumulated frequency distribution shown in Fig. 28, the frequency of fracturing time under constant stress seems to decrease exponentially.

This process is adequately explained stochastically in the following way[38]. When a constant stress is applied at $t=0$, the following probabilities are defined,

$\mu(t)dt$: the probability of transition from the non-fracture state to the fracture state during the following time interval (dt) (The transition prob. of fracture).

$q(t)dt$: the probability of the generation of fractures in any time interval (dt) ($q(t)$ is the probability density function).

$P(t)$: the probability with which the fracturing time becomes larger than t (The accumulated probability density function).

Then, we have

$$P(t)=\int_t^\infty q(t)dt, \tag{9-1}$$

$$q(t)=n(t)/N_0,\quad P(t)=N(t)/N_0, \tag{9-2}$$

where N_0 is the total number of specimens.
So, we have

$$\begin{aligned}\mu(t)\,dt &= -\frac{dP(t)}{dt}\\ &= -d[\log P(\mathrm{t})].\end{aligned} \tag{9-3}$$

Therefore, we get

$$P(t)=\exp\left\{-\int_0^t \mu(t)\,dt\right\}, \tag{9-4}$$

$$q(t)=\mu(t)\exp\left\{-\int_0^t \mu(t)\,dt\right\}, \tag{9-5}$$

where $q(t)$ and $P(t)$ are observable values in the present experiment. Eq. (9-3) indicates that the transition probability $\mu(t)$ is obtained as a gradient of the $\log P(t)-t$ curve. As shown previously in Fig. 28, except for the stage of small t, the relation between $\log N(t)$ and t is approximately linear. Thus, we have

$$\mu=\mu_0, \tag{9-6}$$

$$P(t)=e^{-\mu_0 t}, \tag{9-7}$$

and

$$q(t)=\mu_0 e^{-\mu_0 t}. \tag{9-8}$$

Therefore, it is concluded that the rock fracturing under constant stress occurs with the constant transition probability μ_0.

Furthermore, the transition probability μ_0 depends on the applied stress. To obtain the quantitative relation μ_0 and the applied stress σ, the mean fracturing time t_m is measured under various constant loads,

38) M. HIRATA, *loc. cit.*, 34).

because the mean fracturing time has the following relation with μ_0, that is,

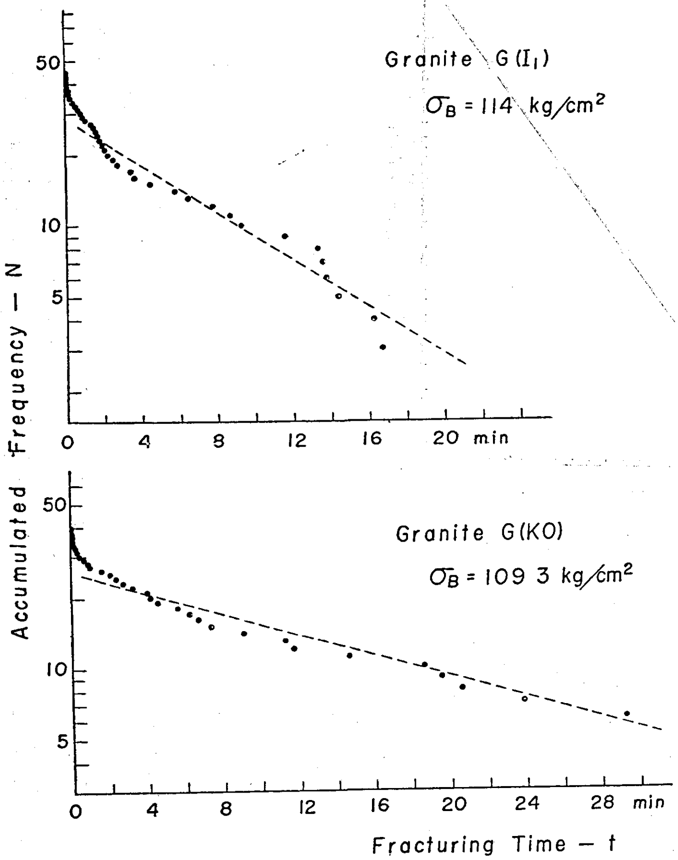

Fig. 28. Accumulated frequency curves of fracturing time of granite specimens under the constant stress. They correspond to the frequency histograms in Fig. 27.

$$t_m = \frac{1}{\mu_0}. \tag{9–9}$$

Thus, the obtained relation between μ_0 (or t_m) and σ is shown in Fig. 29, and so it seems to be expressed by

$$\mu_0 = Ae^{\beta\sigma}, \tag{9–10}$$

where $A = 4.0 \times 10^{-18}\text{min}^{-1}$, and $\beta = 0.37\ \text{cm}^2/\text{kg}$.

Thus, the time characteristics of the generation of fracture in rocks are quantitatively obtained by Eqs. (9–8) and (9–10). Although the above discussion was made for the main rupture of the rock specimen, this process of the occurrences of elastic shocks caused by local fractures of heterogeneous rock specimens is similarly explained by the above mentioned theory. In fact, the frequency of elastic shocks under a constant load decreases also nearly exponentially with time, except in the initial stage (Figs. 24 and 25).

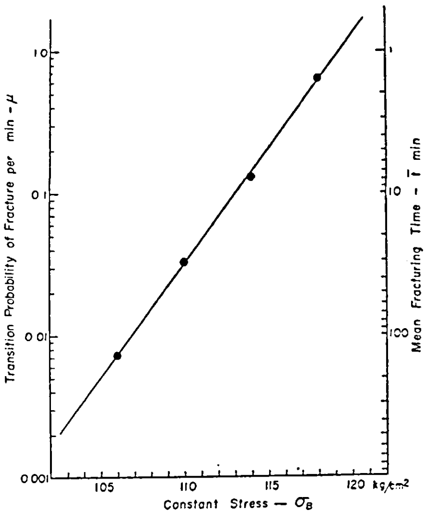

Fig. 29. Relation between the fracturing probability and the applied constant stress for the granite specimens G(I_1).

When μ of each specimen under the stress is *not constant* (or the coefficient of stress concentration in the local fractures fluctuates spatially), the frequency distribution of the fracturing time is also obtained by the superposition of frequency distribution in the cases of *constant* μ. That is, if the distribution function of the transition probability μ is represented by $g(\mu)$, $P(t)$ is calculated as follows,

$$P(t)=\int_{\mu_1}^{\mu_2} g(\mu)\exp\{-\mu t\}\,d\mu. \tag{9–11}$$

According to the result, the graph of the $\log N(t)-t$ relation concaves upward. The departure from the linearity at the initial stage in Figs. 24, 25 and 28 seems to be caused by such variation of the transition probability μ.

Next, when the external stress changes with time, $q(t)$ and $P(t)$ are also obtained by the superposition of those in the cases of constant stress, as follows,

$$\left.\begin{aligned} &\mu(t)=Ae^{\beta\sigma(t)},\\ &q(t)=\mu(t)\exp\left\{-\int_0^t \mu(t)dt\right\},\\ \text{and}\quad &P(t)=\exp\left\{-\int_0^t \mu(t)dt\right\}. \end{aligned}\right\} \tag{9–12}$$

When the stress increases at a constant rate (r), the result is

$$\left.\begin{aligned} &\sigma=rt,\\ &\mu(t)=Ae^{\beta rt},\\ \text{and}\quad &q(t)=\frac{Ae^{\beta\sigma}}{r}\exp\left\{\frac{A}{\beta r}(1-e^{\beta\sigma})\right\}. \end{aligned}\right\} \tag{9–13}$$

The relation between the rate of stress application and the fracture strength of the specimen is derived from the above equations[39]. That is,

$$S=\frac{1}{\mu}\log\left(\frac{\beta r}{A}\right). \tag{9–14}$$

In fact, the experimentally obtained results for granite specimens is

$$S_{compr.}=112\log r+1942\ (\mathrm{kg/cm^2}), \tag{9–15}$$

where r is a rate of stress increase ($\mathrm{kg/cm^2\,sec}$). These relations are

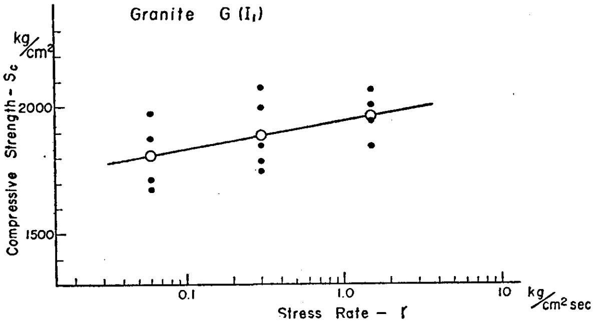

Fig. 30. Relation between the compressive fracture strength and the rate of stress application in the granite specimens $G(I_1)$.

Table 7. Compressive strength of granite specimens ($G(I_1)$) at various stress rates.

Stress rate ($\mathrm{kg/cm^2\,sec}$)	Specimen No.	Compressive strength ($\mathrm{kg/cm^2}$)	Mean ($\mathrm{kg/cm^2}$)
1.5	5 15 25 35	1840 1940 2060 2000	1960±81.2
0.3	9 23 29 33 38	1840 1990 2080 1740 1780	1886±128.9
0.06	4 14 24 34	1870 1970 1710 1670	1805±121.1

39) M. Hori, *loc. cit.*, 37).

considered to be also applicable to the local fractures of rocks (elastic shocks).

According to the above mentioned results, the generation of local fractures in heterogeneous materials is regarded as a sort of stochastic process, and the transition probability has a quantitative relation to the stress state. Therefore, the frequency-time relation is a function of the stress state, as shown in Eqs. (9–12). Thus, the stress is derived from the frequency curve of elastic shocks, in the following way, that is,

$$\sigma(t)=\frac{1}{\beta}\log\left\{-\frac{1}{A}\frac{d}{dt}[\log P(t)]\right\}. \qquad (9\text{–}16)$$

Furthermore, it is easily derived from the above discussion that the frequency distribution of time intervals in a stationary state should be expressed by an exponential function.

10. Time characteristics in the occurrences of elastic shocks (3) —Its relation to earthquakes

The structure of the earth's crust is considered to be remarkably heterogeneous in various scales. When such heterogeneous materials are subjected to external stress, stress concentration at many points appears inside the medium and the local fractures occur at such stress concentrated points. If the earthquakes (of shallow focus) are caused by local fractures in the earth's crust, the generation of earthquakes should be quite analogous to that of the local fractures of heterogeneous medium (namely elastic shocks), and also may be explained as a sort of stochastic process. In fact, statistical results in earthquake phenomena seem to correspond to the experimental results of elastic shocks.

The frequency distribution of time intervals in successive earthquakes was investigated by several investigators[40)41)]. For general earthquakes, we have

$$n(\tau)d\tau=he^{-\alpha\tau}d\tau, \qquad (10\text{–}1)$$

where τ is a time interval and $n(\tau)d\tau$ is the frequency of time intervals between τ and $\tau+d\tau$, and h and α are constants. The distribution function of time intervals is similar to Eq. (8–1) in elastic shocks.

40) S. WATANABE, *Bull. Inst. Phys. Chem. Res.*, **15** (1936), 1083-1085.
41) S. YAMAGUCHI, *Bull. Earthq. Res. Inst.*, **11** (1933), 48-68.

Recently, Y. Tomoda[42] reported that the frequency distribution of the time intervals of aftershocks and volcanic earthquakes were expressed by

$$n(\tau)d\tau = k\tau^{-\nu}d\tau, \tag{10-2}$$

where k and ν are constants. However, these results do not necessarily mean the inapplicability of Eq. (10-1) for these cases. For example, his data on the volcanic earthquakes which originated from Volcano Asama[43] were reconsidered here (Fig. 31). If the period in question is divided into two parts (a) and (b) in which the occurrences of earthquakes seem to be nearly stationary, the frequency distributions of time intervals in each period are clearly expressed by Eq. (10-1) and the exponent α takes quite different values for the two periods, as shown in Fig. 31. Summing up these two different stages, a distribution like Eq. (10-2) seems to be obtained, as

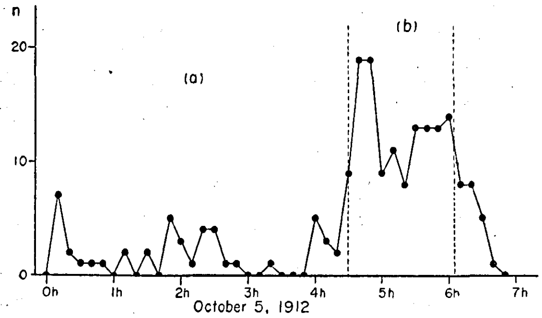

Fig. 31 (I). A frequency curve of volcanic earthquakes in the volcano Asama (after F. Ōmori). (The period (a) begins from October 3, 1912).

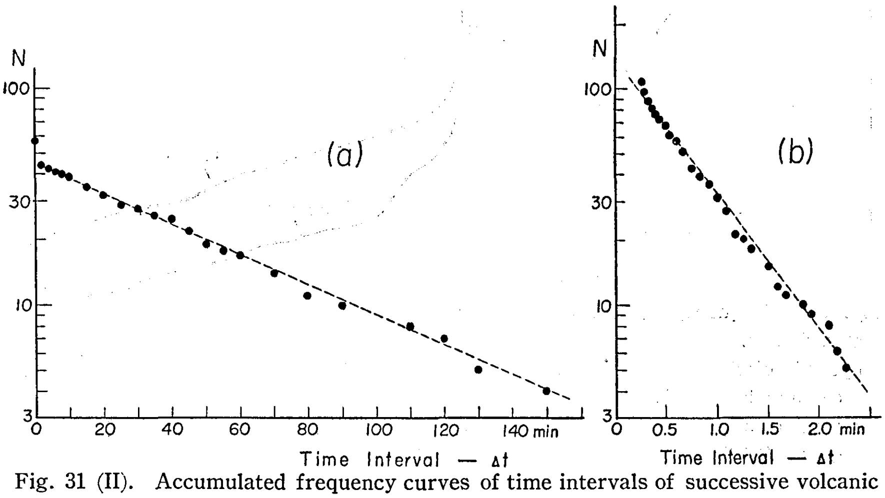

Fig. 31 (II). Accumulated frequency curves of time intervals of successive volcanic earthquakes in each period.

42) Y. TOMODA, *loc. cit.*, 29).

43) F. ŌMORI, *Bull. Imper. Earthq. Inv. Comm.*, **6** (1914), 227-257.

mentioned in the preceding section dealing with elastic shocks. With respect to aftershocks, T. Senshū[44] also suggested a similar result.

Thus, it may be concluded that the exponential function (10–1) is the most fundamental in the frequency distribution of the time intervals of earthquakes and almost all of the observed results seem to be explained by Eq. (10–1) or its superposition. Therefore, earthquakes seem to take place stochastically with a probability which depends on the stress state at the origin.

If the occurrences of earthquakes is regarded as a sort of stochastic process, the frequency curves of earthquakes should have a close relation to the stress state in the earth's crust. As an example, the frequency curves of aftershocks shall be investigated here. It is known that the frequency curve of aftershocks is adequately expressed by the following empirical formula[45)46)],

$$n(t)=E_0 t^{-h}, \quad 0<t<100 \text{ days}, \qquad (10\text{–}3)$$
$$n(t)=n_0 e^{-pt}, \quad t>100 \text{ days}, \qquad (10\text{–}4)$$

where E_0, h, n_0 and p are constants. It is an interesting fact that the accumulated frequency curve of aftershocks is similar to that of the first-class elastic

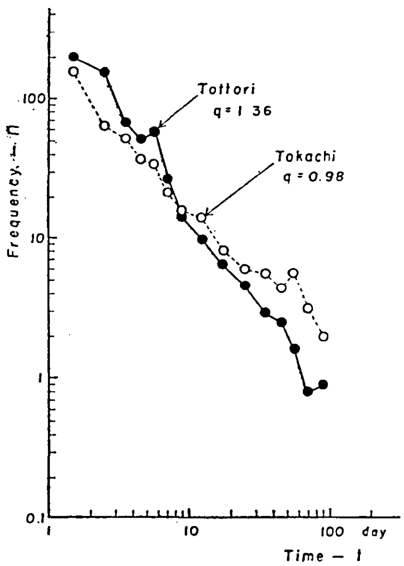

Fig. 32. Frequency curves of aftershocks.
opened circle: Off Tokachi earthquake (1952).
closed circle: Tottori earthquake (1943).

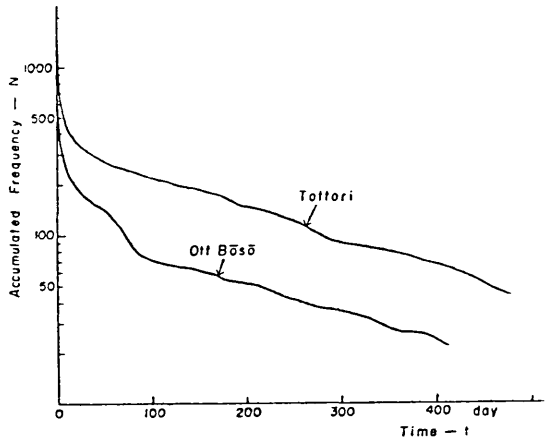

Fig. 33. Accumulated frequency curves of aftershocks.

44) T. SENSHŪ, *Zisin* (*Journ. Seis. Soc. Japan*), [ii], **12** (1959), 149-161.
45) T. UTSU, *Zisin* (*Journ. Seis. Soc. Japan*), [ii], **10** (1957), 35-45.
46) K. MOGI, *Bull. Earthq. Res. Inst.*, **40** (1962), 107-124.

shocks in heterogeneous materials under a constant stress, although the time scale is very different in both cases (Fig. 33). If the relation Eq. (9–15) is applied to the frequency curve of aftershocks, the relation for the change of stress in the aftershock region is derived (see Fig. 34). According to this result, the mean stress in the aftershock region decreases exponentially after the main shock and converges to a constant value after several tens of days. That is, it seems to be represented by

$$\sigma(t)=\sigma_0+\sigma_1 e^{-\gamma t}, \qquad (10\text{–}5)$$

where σ_0, σ_1 and γ are constants.

Thus, if the fracturing characteristics of the earth's crust are assumed, the state of stress will be approximately deduced from the frequency curves of earthquakes originating from the region. Therefore, the change in stress before the major earthquake may be also obtained from the observation of minor earthquakes in the region.

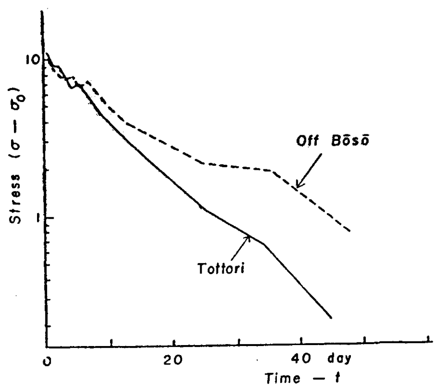

Fig. 34. Changes of estimated stress in the aftershock regions. The scale of stress is conventional.

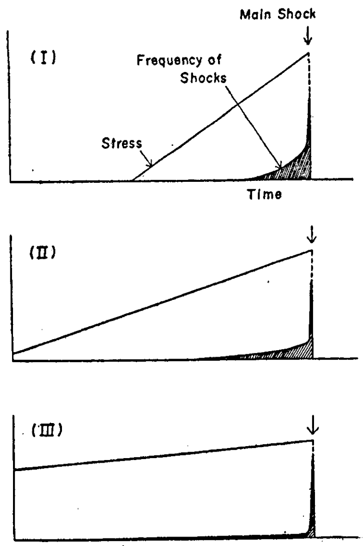

Fig. 35. Generation of before-shocks.
(I): the stress rate is large.
(II): the stress rate is medium.
(III): the stress rate is small.

If the main earthquakes are caused by the fracturing of the earth's crust (a heterogeneous material) under increasing stress, a number of minor beforeshocks shall take place in the stressed region. However, their frequency per unit time depends on the rate of stress increase, so that the frequency of beforeshocks per unit time may be remarkably small, if the applied stress increases very gradually.

11. Summary and acknowledgement

The main results of this study on elastic shocks may be summarized as follows:

(1) When increasing stress is applied to various brittle materials, elastic shocks begin to occur at some stress state, and they increase generally with the increasing stress. Elastic shocks occur more frequently with the increasing degree of heterogeneity.

(2) Under the application of a constant stress to the heterogeneous medium, a large number of elastic shocks occurs, and immediately they begin to decrease gradually, and after some duration, again they begin to increase before the occurrence of the main rupture.

(3) It is important that elastic shocks increase remarkably preceding a main rupture of a heterogeneous medium both under increasing stress and constant stress.

(4) The observation of elastic shocks in the processes of deformation seems to give a clue to clarifying the machanism of the non-elastic deformation of rocks and other heterogeneous materials. Thus, a suggestion as to the mechanism of rock creep may be obtained.

(5) Based on the total energy of elastic shocks, the degree of brittleness of heterogeneous materials was defined as

$$B=\frac{2W_{ef}}{\epsilon_n S}.$$

According to this definition, granite is highly brittle as compared with andesite.

(6) In the heterogeneous materials, such as natural rock specimens, the magnitude distribution of elastic shocks satisfies the following equation which is named Ishimoto-Iida's empirical formula,

$$n(a)da=n_0a^{-m}da.$$

The exponent m increases with the degree of heterogeneity and furthermore with the degree of spatial variation in the stress distribution. That is, the exponent m in the pumice samples which are extremely heterogeneous is very large (2～3) and on the other hand, it is very small in a homogeneous medium, such as pine resin, under a uniform stress.

(7) The elastic shocks occur stochastically with a transition probability which depends on the stress state. Therefore, the frequency curve of elastic shocks under a constant stress is expressed by an exponential function, and the frequency distribution of time interval in a stationary process is expressed by an exponential function. This was ascertained for the rock specimens.

(8) From the above mentioned relation between the transition probability and the applied stress, the frequency curves of elastic shocks under variable stress were calculated theoretically.

In considering earthquakes, if they be the elastic waves of shock type caused by the brittle fracturing of the earth's crust, some of the above mentioned results concerning experimental elastic shocks should be applied to some problems in earthquakes. The main results may be summarized as follows:

(9) From the fact that the magnitude distribution of earthquakes is well expressed by Ishimoto-Iida's empirical formula and the exponent m in the equation is nearly constant in various general earthquakes, it was deduced that the mechanical structure of the earth's crust is appreciably heterogeneous and the degree of heterogeneity is nearly similar in any parts of the earth's crust, if the applied stress be assumed to be comparatively uniform. Furthermore, it is suggestive, concerning the heterogeneity of the earth's crust, that their exponent m is nearly equal to that of the elastic shocks in crystalline rocks.

(10) The extremely large values of the exponent ($m=2\sim4$) in volcanic earthquakes of very shallow origin indicate that the variation in stress distribution in the crater bottom of an active volcano will be extremely large. The stress state seems to be caused both by the remarkable heterogeneity of material in the region and the concentration of the applied stress at the crater bottom.

(11) If the process of the occurrence of earthquakes is regarded as stochastic like that of elastic shocks, as we have already assumed, the relation between the frequency of earthquakes in the region and the stress state should be also estimated under some assumptions. Thus, as examples, the change in the stress state in the aftershock region after the main shock was estimated from the above relation. Then, it was also deduced that the minor shocks increased preceding the main

shock, corresponding to experimental elastic shocks. However, it is questionable whether or not they are always observable using the present seismometric methods.

Furthermore, it was derived that the frequency distribution of time intervals of successive earthquakes in stationary states could be explained by the exponential function.

The writer wishes to express his sincere thanks to Professor T. Minakami for his many kind advices and encouragements. The writer also wishes to express his heartful thanks to Professor C. Tsuboi for his valuable advices and suggestions. Further, the writer's thanks are also due to Dr. N. Yamakawa for his helpful discussions, and Dr. S. Nagumo, Dr. J. Ossaka and Mr. T. Watanabe for their kind help to carry out his experiment.

6. 不均質媒質の破壊に伴う Elastic Shocks の発生及びそれに関連した地震現象の二，三の問題の研究

地震研究所 茂 木 清 夫

地殻に作用する歪力に因る地殻の急激な破壊乃至はそれに類似した現象に伴つて地震が発生するという考えは，(比較的浅い) 地震の原因として多くの研究者に支持されているように思われる．このような観点から地震現象を見るならば，地殻の破壊特性を明らかにすることが，地震発生の諸問題を解く重要な手掛りとなると考えられる．本論は，このような立場から，地殻の破壊に関する性質に類似すると思われる不均質媒質の破壊特性を実験的に研究して，地震現象を明らかにする手掛りを得ようと試みたものである．

地殻の破壊に関する性質を特徴づける重要な要素として，まず脆性と構造的不均一性があげられる．従つて，上述の目的のためには，これらの性質に着目して，破壊の諸性質を調べることが有益な結果を与えると考えられる．そこで今回は，種々の不均質度をもつ脆性媒質として，軽石，結晶質岩石，およびガラス等をとり，一様等速増加応力および一定持続荷重を加えた場合に生ずる破壊群，とくにそれに伴つた Elastic Shocks (衝撃性弾性波) の発生過程およびその大きさ分布を，主として統計的に研究したが，次にその結果を要約する．

(1) 花崗岩や軽石のような不均質脆性媒質に比較的一様な等速増加応力を加えた場合，応力の増加と共に Elastic Shocks が著しく発生する．これに対して，安山岩のうちの A(K_1) やガラスおよび松脂等の均質な媒質では，試験体の全面的破断に至るまで，Elastic Shocks の発生は極めて少ないかまたは全く認められない．上述のような Elastic Shocks の頻発は不均質脆性媒質の特性である．

(2) 不均質脆性媒質に一定持続応力を作用させた場合に，直ちに Elastic Shocks が頻発し，以後次第に減少する．ただし，試料の巨視的破砕（または破断）の発生の直前に再び著しい増加を示す．一定応力下のこのような現象もまた不均質脆性体に特有である．

(3) 岩石試料の一定荷重のもとにおける Elastic Shocks の発生経過は，岩石の creep の機構を明らかにする一つの手掛りを与える．即ち，transient creep の機構が高圧実験の結果から岩石内の微小破壊によると推定されたが (E. C. Robertson), Elastic Shocks の測定の結果，このような微小破壊群の発生が直接確められた．なお，一般に Elastic Shocks の測定は，媒質内の破壊発生を探知する有力な手段となり得る．

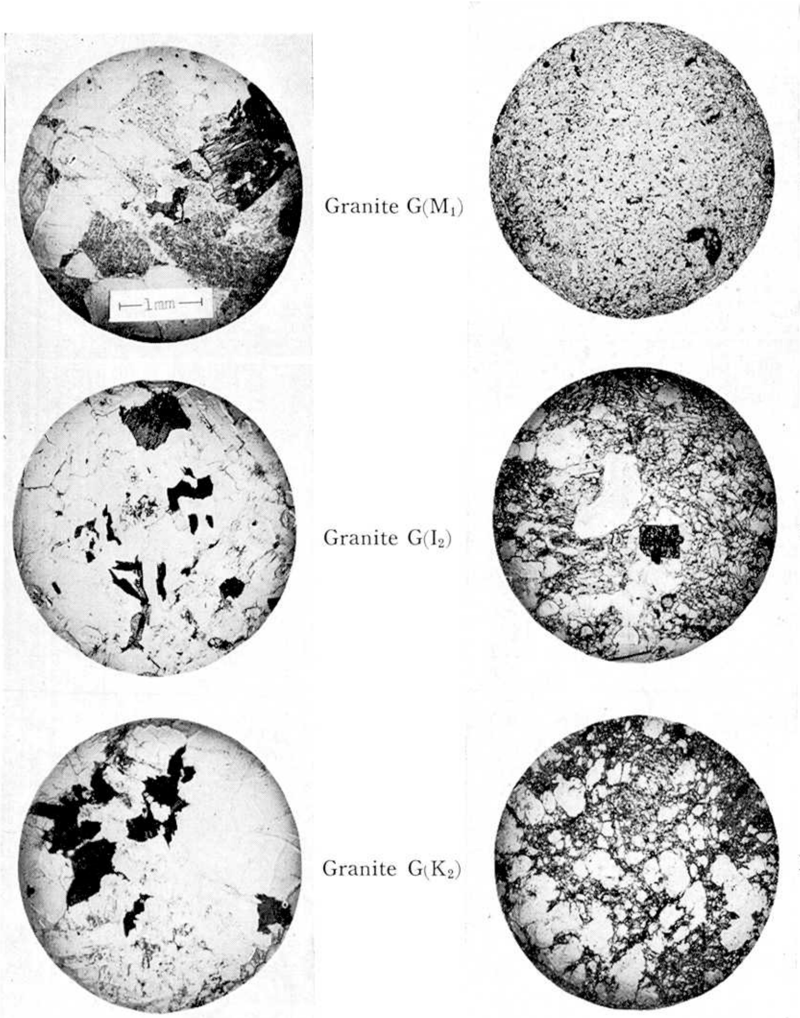

Fig. 36. Micro-photographs of test specimens.

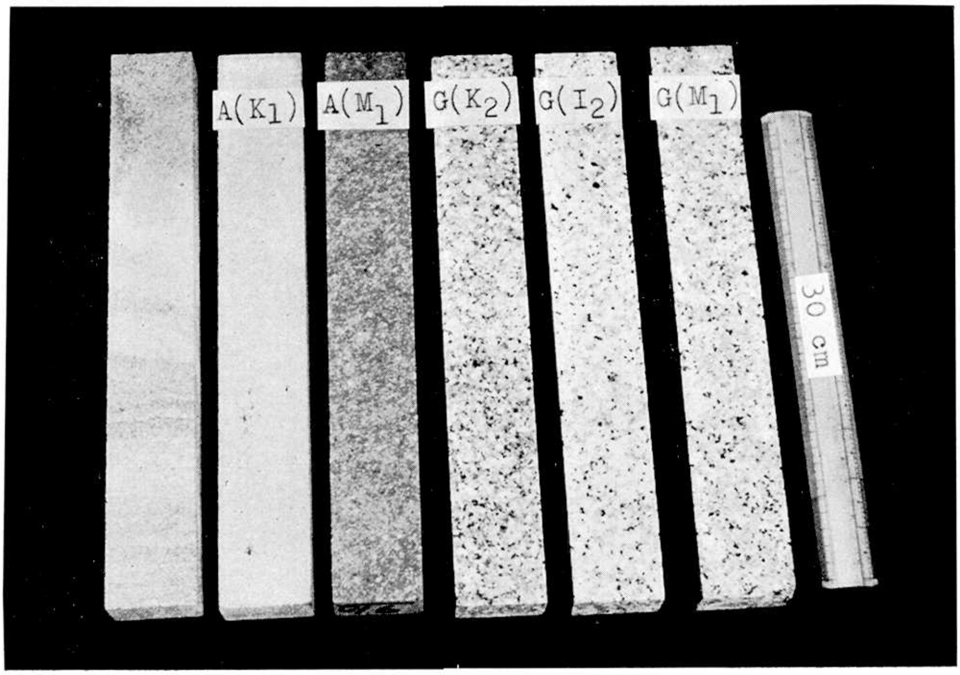

Fig. 37. Rock specimens for bending test.

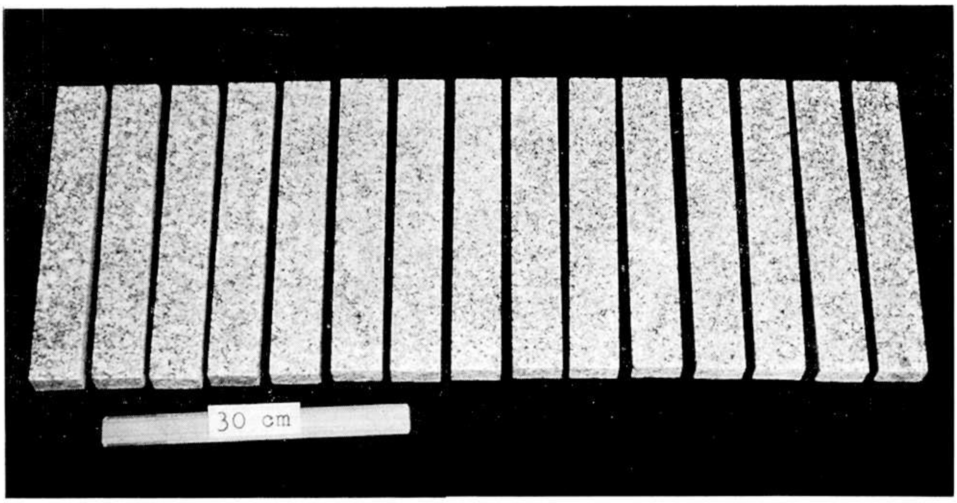

Fig. 38. Granite G(K_2) specimens.

(震研彙報 第四十号 図版 茂木)

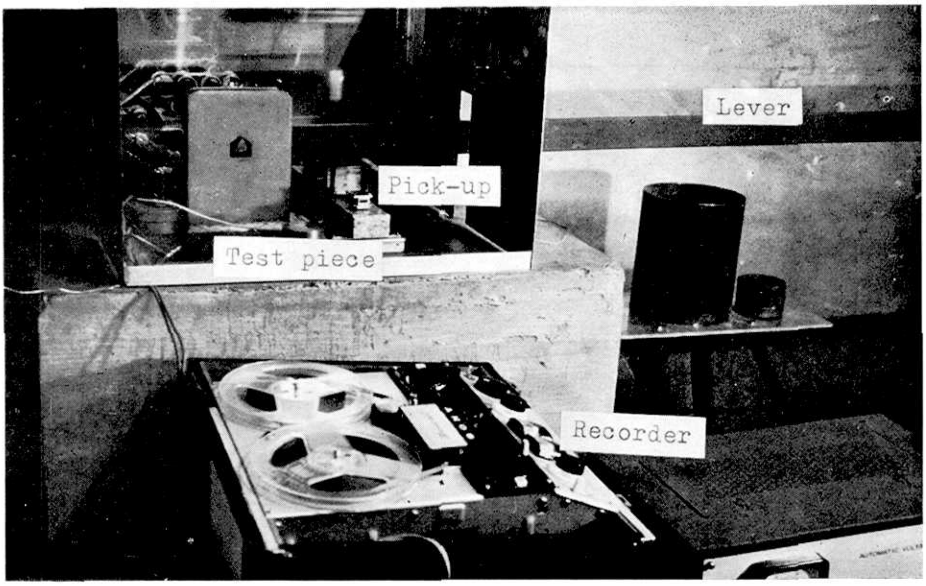

Fig. 39. Apparatus for shock measurement.

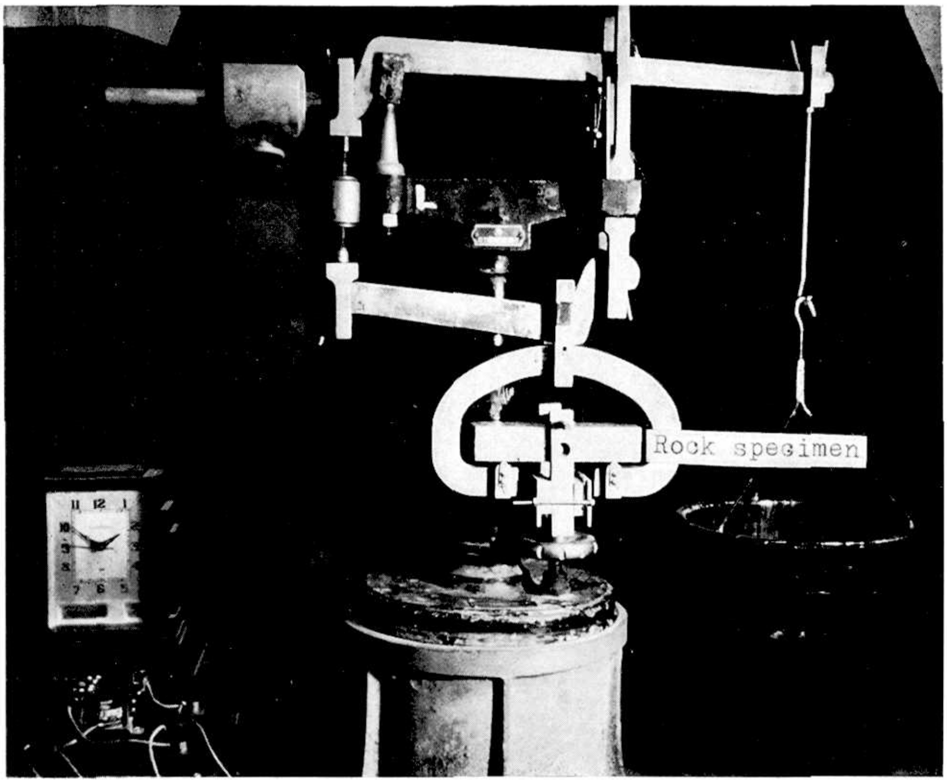

Fig. 40. Michaelis bending apparatus.

(4) Elastic Shocks の発生は媒質の脆性破壊に因るものであることから，次のような量をもつて不均質媒質の脆性度の尺度とすることができる．

$$B=\frac{2W_{ef}}{S\cdot\varepsilon_n}$$

それによると，花崗岩は一般に安山岩よりも著しく脆性的である．

(5) 軽石，花崗岩および安山岩等の破壊に伴つた Elastic Shocks の大きさ分布はほぼ一定の統計法則に従つている．即ち，その最大振巾に関しては，地震で知られている石本・飯田の統計式が適用され，結晶質岩石試料では，その指数mが 1.5～2.0 で一般の地震の場合に類似し，また不均質度の著しく高い軽石では，指数mが明らかに大きい値 (2～3) を示す．均一応力のもとでの均質媒質では，微小破壊は発生しがたく，このような分布とは異つている（或いはmが著しく小さい傾向を示す）．このように均一な応力のもとで石本・飯田の統計式が成立し，指数mが如何なる値をとるかは，媒質の不均質度に関係するもので，不均質度が著しいほど指数mの値が大きい傾向が認められる．

(6) 均質媒質に不均一応力が作用した場合にも石本・飯田の統計式が成り立つ場合があることから，この統計式の成立は媒質内の応力分布の不均一性に関係すると考えられる．この結果にもとづいて，二，三の仮定のもとに石本・飯田の統計式を導びいた．それによれば，指数mは媒質内の応力分布の不均一度と共に増加する．

(7) Elastic Shocks の時間間隔の頻度分布は，定常状態では指数分布を示す．任意の過程もそれをいくつかの定常的過程に分ければ，それぞれについて指数分布を示す．

(8) 一定持続応力のもとでの Elastic Shocks の頻度は，初期の段階をのぞけば，凡そ指数函数的に減少する．従つて，一定応力状態のもとでは，一定の遷移確率をもつて発生すると考えられる．

(9) Elastic Shocks のこのような時間特性は，一種の確率過程としてよく説明される．このような発生特性を定量的に調べるために，応力分布の一層明確な，巨視的破断について，破壊時間を測定して，その発生確率と応力との関係を求めた．このような試料の巨視的破断の発生も，またその局部的破壊群（即ち Elastic Shocks）の発生も確率過程論的破壊論によつて説明される．この結果にもとづいて，Elastic Shocks の頻度曲線と応力状態との関係が求められる．

次に，地殻が不均質脆性媒質であり，地震はその局部的破壊に伴う弾性波であると考えれば，これらの Elastic Shocks に関して得られた結果の多くが，地震の場合に適用され，次のような結果が導かれる．

(10) Elastic Shocks の大きさ分布に関する上述の結果を地震に適用すれば，地震の場合に石本・飯田の統計式が成立し，指数mが 1.5～2.0 であることは，地殻ではある程度応力が不均一に分布していること，そしてそれが結晶質岩石に応力が作用した場合の内部の応力分布の不均一さと類似の程度（但し長さの尺度が非常にちがう）であることを示している．

(11) 火山地震のうちやや深い所に発生する地震では指数mが 1.5～2.0 程度で一般の地震と同程度の値を示すが，活動的な火山の火口直下の極く浅い所に発生する地震ではmが著しく大きい値 (2～4) を示す．これは，火口直下の浅い部分では，媒質が極度に不均質状態にあり，また作用する応力も不均一に集中的に作用するためであると考えられ，一方やや深い部分では，他の地殻の部分と大差のないことを示すものと考えられる．

(12) 地殻に外応力が作用した場合に発生する地震の時間特性は，上述の Elastic Shocks のそれに対応するものと考えられる．例えば，定常状態における時間間隔の分布はやはり指数分布で表わされる．

(13) 若干の仮定のもとに，地震の頻度曲線から地殻の応力の変化状態が推定される可能性がある．一例として，余震の場合を取扱つたが，余震域の応力は本震後急激に減少し，次第に一定値に近づくことが推定された．